16

Fluorophores for Confocal Microscopy: Photophysics and Photochemistry

Roger Y. Tsien, Lauren Ernst, and Alan Waggoner

INTRODUCTION

Fluorescence is probably the most important optical readout mode in biological confocal microscopy because it can be much more sensitive and specific than absorbance or reflectance, and because it works well with epi-illumination, which greatly simplifies scanner design. These advantages of fluorescence are critically dependent on suitable fluorophores that can be tagged onto biological macromolecules to show their location, or whose optical properties are sensitive to the local environment. Despite the pivotal importance of good fluorophores, little is known about how rationally to design good ones. Whereas the concept of confocal microscopy is only a few decades old and nearly all the optical, electronic, and computer components to support it have been developed or redesigned in the last few years, the most popular fluorophores were developed more than a century ago (in the case of fluoresceins or rhodamines) or several billion years ago [in the case of phycobiliproteins and green fluorescent proteins (GFPs)]. Moreover, whereas competition between commercial makers of confocal microscopes stimulates ardent efforts to refine the instrumentation, relatively few companies or academic scientists are interested in improving fluorophores.

PHOTOPHYSICAL PROBLEMS RELATED TO HIGH INTENSITY EXCITATION

Singlet State Saturation

The properties of current fluorescent probes relevant to conventional fluorescence microscopy have been reviewed recently (e.g., Waggoner *et al.*, 1989; Tsien, 1989a,b; Chen and Scott, 1985; Sun *et al.*, 2004; Johnson, Chapter 17, *this volume*) and are listed in Table 16.1, see p. 344. Absorption spectra of several representative fluorescent probes in relation to the common laser line wavelengths available for confocal laser scanning microscopes are presented in Figure 16.1. Confocal microscopy using multiple apertures scanned across an image plane, that is, disk-scanning confocal microscopy, is essentially similar to conventional microscopy in its requirements on fluorophores. By contrast, continuous beam (not pulsed as in multi-photon excitation) laser-scanning microscopy subjects each fluorescent molecule to brief but extremely intense bursts of excitation as the focused laser beam sweeps past. If the laser-scanned image consists of n pixels (typically $n > 10^5$), any one pixel is illuminated for $1/n$ of the total time, or even somewhat less if some of the cycle time must be devoted to scan retrace; therefore, the peak instantaneous intensity must equal or exceed n times the long-term average excitation intensity.

Some idea of the quantitative magnitude may be gathered from the following example, analogous to that discussed by White and Stryer (1987). If just 1 mW of power at the popular 488 nm line of the argon-ion laser is focused to a Gaussian spot whose radius w at $1/e^2$ intensity is 0.25 µm, as is achieved by a microscope objective of 1.25 numerical aperture (Schneider and Webb, 1981), the peak excitation intensity I at the center will be $10^{-3}\,\mathrm{W}/[\mathrm{p} \cdot (0.25 \times 10^{-4}\,\mathrm{cm})^2] = 5.1 \times 10^5\,\mathrm{W/cm^2}$, or about 1.25×10^{24} photons/($\mathrm{cm^2} - \mathrm{s}$). Such intensities are well able to excite fluorophores so rapidly that few molecules are left in the ground state and the population is emitting photons nearly as fast as the limit set by the excited-state lifetime. For example, if fluorescein is the fluorophore, its decadic extinction coefficient ε at 488 nm is about $80{,}000\,\mathrm{L \cdot mole^{-1} cm^{-1}}$ at pH > 7. To convert this to the optical cross-section per molecule, one must multiply ε by $(1000\,\mathrm{cm^3/L}) \cdot (\ln 10)/(6.023 \times 10^{23}$ molecules/mole$) = 3.82 \times 10^{-21}\,\mathrm{cm^3 \cdot mole \cdot L^{-1} \cdot molecule^{-1}}$, giving a cross-section s of $3.06 \times 10^{-16}\,\mathrm{cm^2/molecule}$. In a beam of 1.25×10^{24} photons $\cdot\,\mathrm{cm^{-2} s^{-1}}$, each ground state molecule will be excited with a rate constant $k_a = \sigma I$, or $3.8 \times 10^8\,\mathrm{s^{-1}}$ in this example. The excited state lifetime τ_f of fluorescein in free aqueous solution is known to be about 4.5 ns (Bailey and Rollefson, 1953), which means that molecules in the excited state return to the ground state with a rate constant k_f of $2.2 \times 10^8\,\mathrm{s^{-1}}$. Note that k_f is defined here as the composite rate constant for all means of depopulating the singlet excited state, the sum of the rate constants for fluorescence emission, radiationless internal conversion, intersystem crossing to the triplet, etc.

Because of the Stokes shift between excitation and emission λs, k_f is not significantly enhanced by stimulated emission effects. If x is the fraction of molecules in the excited state and $(1 - x)$ is the fraction in the ground state, at steady-state $k_f x = k_a(1 - x)$. Solving for x yields the equation $x = k_a/(k_a + k_f)$, which shows that in this example 63% of the fluorescein molecules would be in the excited state and only 37% in the ground state. Obviously the emission is nearly saturated, and further increase in excitation intensity could hardly increase the output. The actual rate of photon output per molecule is $Q_e k_f x = Q_e k_f k_a/(k_a + k_f)$, where Q_e is the emission quantum efficiency, about 0.9 for free fluorescein dianion (but usually less for fluorescein bound to proteins, see below).

In this example each molecule would be emitting at an average rate of 1.3×10^8 photons/s, close to the absolute maximum of $Q_e k_f$ of about 2×10^8 photons/s. In current typical scanning confocal

Roger Y. Tsien • School of Medicine, University of California, San Diego, California 92093
Lauren Ernst and Alan Waggoner • Carnegie Mellon University, Pittsburgh, Pennsylvania 15213

 Handbook of Biological Confocal Microscopy, Third Edition, edited by James B. Pawley, Springer Science+Business Media, LLC, New York, 2006.

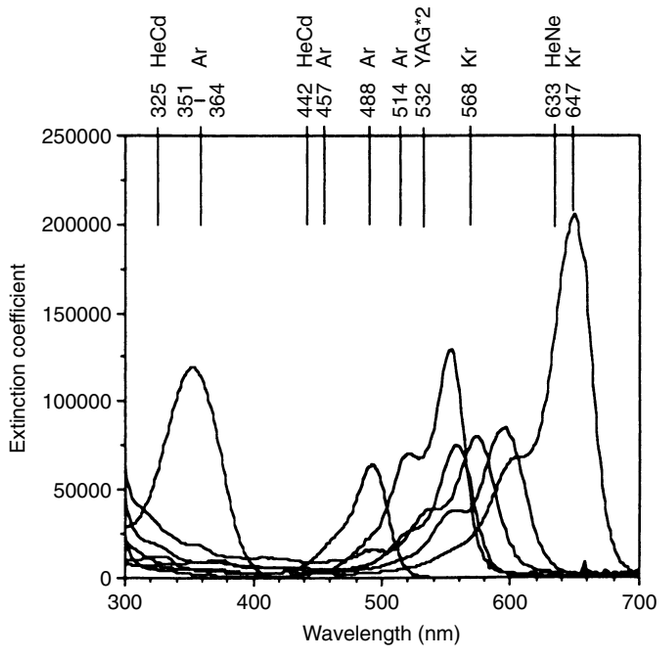

FIGURE 16.1. Absorption spectra from left to right of Hoechst 33342+DNA, and Fluorescein, CY3, TRITC, Lissamine Rhodamine B, Texas Red, and CY5 conjugated to antibodies. Extinction coefficients are given on a per-dye basis. Common laser emission λs are presented at the top of the figure. λs in bold are for the lower power, less expensive lasers, which provide sufficient excitation intensity for most fluorochromes imaged with laser-scanning microscopes with higher power objectives.

microscopes, the beam dwells on each pixel for 1 to 10 µs, so one would expect each molecule to produce several hundred photons. However, only a minority enter the microscope objective, only a fraction of these manage to pass all the way through the scanner optics, and only 10% to 20% of these create photoelectrons in the photomultiplier cathode, so that each molecule probably contributes on the order of only one photoelectron/pixel/sweep. Because of fluorescence saturation, increasing the laser power will not significantly increase the signal amplitude. In reality, it is difficult to accurately predict the laser power at which a fluorophore will saturate. Accurate knowledge of the extinction coefficient at the λ of excitation and the excited state lifetime of the fluorophore is essential but not always easy to obtain. Coumarins, for example (Table 16.1, see p. 344), have extinction coefficients approximately 2 to 5 times smaller than the fluoresceins, rhodamines, and cyanines, and would be expected on this basis alone to require a 2- to 5-fold increase in laser power before saturation. However, the emission lifetimes of coumarins are intrinsically longer than those of the fluoresceins, rhodamines, and cyanines, so that the factor of 2 to 5 is not realized in practice. To make calculations more difficult, the extinction coefficients and the excited state lifetimes of most probes depend on the environment of the fluorophore. For example, increasing the fluorochrome-to-protein ratio of a labeled antibody from 2 to 5 can reduce the average excited state lifetime of the bound fluorochromes several-fold. For these reasons, the power saturation values for the probes listed in Table 16.1 are not given. However, as a general rule, fluorochromes with extinction coefficients and quantum efficiencies similar to fluorescein will also saturate under similar conditions.

Triplet State Saturation

The above calculation considers only the ground state and lowest excited singlet state. Saturation of emission could occur at even lower excitation intensities if a significant population of fluorophores becomes trapped in a relatively long-lived triplet state. This would take place if a significant quantum yield exists for singlet-to-triplet conversion, or intersystem crossing. For example, if ground-state fluorescein molecules each absorb 3.8×10^8 photons $\cdot$ s^{-1}, have an excited singlet lifetime of 4.5 ns, cross to the triplet state with a quantum efficiency Q_{ISC} of 0.03 (Gandin *et al.*, 1983) and reside in the triplet state for a mean time τ_T of 10^{-6} s, the triplet state would contain 81% of the fluorophore population at steady state, which would be attained with a time constant of about $[\tau_T^{-1} + Q_{ISC}k_f k_a/(k_a + k_f)]^{-1}$ or about 190 ns in this case. Only 12% and 7% would be left in the first excited singlet and ground states, respectively, at steady state, so that the fluorescence emission would be weakened about 5-fold compared to its initial value just after the illumination began but before significant triplet occupancy had built up. Therefore, if the dwell time/pixel is comparable to or greater than the triplet lifetime, then a severe reduction in output intensity may be expected beyond that due simply to the finite rate of emission from the singlet state.

In the above calculation, the most uncertain figure is that for the triplet lifetime τ_T; in very thoroughly deoxygenated solution, τ_T for the fluorescein dianion is 20 ms (Lindqvist, 1960), but oxygen is expected to shorten τ_T down to the 0.1 to 1 µs range. The rate at which different fluorophore environments in a sample quench triplet states and reduce τ_T will of course affect the extent of triplet-state saturation and the apparent brightness of each pixel at these high illumination levels. When τ_T is long, triplet-state saturation is easily attained even without laser illumination (Lewis *et al.*, 1941).

Contaminating Background Signals

Rayleigh and Raman Scattering

Meanwhile, there may be unwanted signals, such as Rayleigh scattering, due either to excitation λs leaking through the dichroic mirror and barrier filter or to imperfect monochromaticity of the excitation source, for example, if the laser is being run in multi-line mode with only an interference filter to select one line. Even if all the λ filtering is perfect, Raman scattering will contribute a fluorescence-like signal, for example, at a λ of $[\lambda_{exc}^{-1} - 3380\,cm^{-1}]^{-1}$ due to the characteristic 3380 cm^{-1} Raman band of water. For an exciting λ_{exc} of 488 nm, the Raman peak would appear at 584 nm. At high concentrations of protein or embedding media, additional Raman bands closer to the excitation wavelength might appear. Both Rayleigh and Raman scattering are directly proportional to the laser power and will **not** saturate as the desired fluorescence does, so that excessive laser power diminishes the contrast between fluorescence and such scattering signals.

Autofluorescence from Endogenous Fluorophores

Another major source of unwanted background is autofluorescence from endogenous fluorophores. Flavins and flavoproteins absorb strongly at 488 nm and emit in the same spectral region as fluorescein. Reduced pyridine nucleotides (NADH, NADPH) and lipofuscin pigments absorb light from ultraviolet (UV) laser lines. These fluorophores usually have lower extinction coefficients or shorter fluorescence lifetimes than most exogenous fluorophores. For example, FMN (flavin mononucleotide) and FAD (flavin

adenine dinucleotide) have the extinction coefficients of 1.1 to 1.2 $\times 10^4\,M^{-1}\,cm^{-1}$ at 445 to 450 nm (Koziol, 1971) and fluorescence lifetimes of about 4.9 and 3.4/0.12 ns, respectively (Lakowicz, 1989), whereas NADH has an extinction coefficient of $6.2 \times 10^3\,M^{-1}\,cm^{-1}$ at its 340 nm peak (Kaplan, 1960) and a lifetime of about 0.4 ns (Lakowicz, 1983). Therefore autofluorescence from these molecules will be more difficult to saturate than the fluorescence from most of the common probes. See Chapter 27, *this volume*, for more on confocal lifetime.

What Is the Optimal Intensity?

The above discussion shows that if laser power is increased to nearly saturate the desired fluorophores, autofluorescence as well as Rayleigh and Raman scattering will increase background levels and decrease the overall signal-to-noise ratio (S/N). What is the optimal intensity? Assuming the system is limited by photon-counting statistics, the irreducible noise level N is proportional to the square root of the background signal level B. Both B and the absorption rate constant k_a of the desired probe are directly proportional to the illumination intensity I and to each other. Therefore N is directly proportional to $k_a^{1/2}$. If triplet state saturation can be ignored, for example, if the dwell time/pixel is short compared to the time for the triplet state to build up, then the desired signal is $Q_e k_f k_a/(k_a + k_f)$ as derived above, so that S/N is proportional to $k_a^{1/2}/(k_a + k_f)$. Regardless of the proportionality constant, this expression is maximal when $k_a = k_f$. This is a remarkably simple but important result, for which we are grateful to Prof. R. Mathies (University of California–Berkeley).

At the other extreme, once the ground state and excited singlet and triplet have all come to an equilibrium steady state, the desired signal is readily calculated to be

$$Q_e k_a/[1 + k_a\,(k_f^{-1} + Q_{ISC}\tau_T)]$$

so that the S/N is proportional to

$$Q_e k_a^{1/2}/[1 + k_a\,(k_f^3 + Q_{ISC}\tau_T)].$$

This reaches its maximum when $k_a(\tau_f + Q_{ISC}\tau_T) = 1$, where $\tau_f = k_f^{-1}$ is the lifetime of the excited singlet. In this approximation, appropriate for slow scans in which the dwell time/pixel is long compared to the time for triplet state equilibration, the laser power P in photons/s should be optimal at about $\pi w^2/[(3.82 \times 10^{-21}\,cm^3 \cdot M)\,\varepsilon\,(\tau_f + Q_{ISC}\tau_T)]$. For the present values of $w = 2.5 \times 10^{-5}$ cm, $\varepsilon = 8 \times 10^4\,M^{-1}\,cm^{-1}$, $\tau_f = 4.5 \times 10^{-9}$ sec, $Q_{ISC} = 0.03$, and $\tau_T = 10^{-6}$ s, this expression gives an optimal P of 1.86×10^{14} photons/s, or about 76 µW at 488 nm. If triplet formation could be neglected, the optimal P would be 590 µW, slightly less than the 1 mW initially postulated to be the input.

PHOTODESTRUCTION OF FLUOROPHORES AND BIOLOGICAL SPECIMENS

One obvious way to increase the total signal is to integrate for a longer time, either by slowing the scan, or by averaging for many scans. Given that image processors are now relatively cheap, the latter alternative is likely to be the easier to implement, and it has at least two major advantages: repetitive scans give time for triplet states to decay between each scan, and the user can watch the S/N gradually improve and choose when to stop accumulating. However, irreversible photochemical side effects such as bleaching of the fluorophore or damage to the specimen set limits on the useful duration of observation or total photon dose allowable. Photochemical damage is one of the most important yet least understood aspects of the use of fluorescence in biology; in this discussion we can do little more than define our ignorance.

At intensities of up to 3×10^{22} (Hirschfeld, 1976) or 4.4×10^{23} photons $\cdot\,cm^{-2} \cdot s^{-1}$ (Mathies and Stryer, 1986), fluorescein is known to bleach with a quantum efficiency Q_b of about 3×10^{-5}. If this value continues to hold at the somewhat higher intensity of the above example, the molecules would be bleaching with a rate constant of $Q_b k_f k_a/(k_a + k_f)$, or about $4.2 \times 10^3\,s^{-1}$. This would mean that 1/e or 37% of the molecules would be left after 240 µs of actual irradiation. The corresponding number of scans would be 240 µs divided by the dwell time that the beam actually spends on each pixel. The average number of photons emitted by a fluorophore before it bleaches is the ratio of emission quantum efficiency to bleaching quantum efficiency, or Q_e/Q_b; this is generally true regardless of whether the illumination is steady or pulsed. For fluorescein under ideal conditions, the above Q_e/Q_b works out to 30,000 to 40,000 photons ultimately emitted/dye molecule (Hirschfeld, 1976; Mathies and Stryer, 1986). The number of photons detected from each molecule will, of course, be considerably less.

Thus, in obtaining an image at a single plane by averaging say 16 scans, one would expect from 6% to 50% bleaching of a fluorescein signal (in the absence of antifade reagents), resulting from exp[–(16 sweeps) × (1–10 µs dwell time/sweep)/(240 µs lifetime)]. In an optical sectioning experiment, the cone of light illuminating the sample above and below each plane of data being acquired is causing photobleaching even though under confocal conditions no signal is being recorded from these regions. This means that if 16 optical sections are obtained with only one sweep each, the last image will have been bleached 10% to 50% by the preceding sweeps. If the signals are large, it may be possible for software to adjust the intensities of sequential images to compensate for bleaching. Of course, for quantitative fluorescence measurements it would be most desirable to use the most bleach-resistant fluorophores available.

Dependency on Intensity or Its Time Integral?

Theory

One major uncertainty is whether the bleaching quantum efficiency Q_b really does remain constant even at such high instantaneous excitation intensities. Theoretically, Q_b could rise at high intensities due to multi-photon absorptions. For example, the normal excited singlet or triplet state could itself absorb one or more additional photons to extra-high energy states, which will probably have picosecond lifetimes. If their main reaction pathway were back to the lowest excited state, then such higher-order states would be innocuous, but if bond dissociation competes with decay to the lowest excited state, then photodestruction will rise steeply as intensities reach levels that significantly deplete the ground state (as in the previous example).

One can also imagine the opposite dependency: bleaching mechanisms whose quantum efficiency might decrease when the excitation was bunched into brief intense pulses. For example, suppose the dye is bleached by a 1 : 1 reaction of its excited state with a molecule of oxygen, and that the overall dye concentration exceeds the oxygen concentration. Then within the zone of intense illumination, the first few excited dye molecules might react with all the locally available O_2, and the resulting anoxic environment would protect the rest of the excited molecules. Oxygen would be diffusing in from the surrounding non-illuminated environment, but the time required would be on the order of the spot radius squared

divided by the diffusion constant, that is, $(0.25 \times 10^{-4}\,\text{cm})^2/(3 \times 10^{-5}\,\text{cm}^2 \cdot \text{s}^{-1})$ or 20 µs, that is, considerably longer than the time for the beam to move to the next pixel. By contrast, with low-intensity illumination, no local anoxia would develop, and each fluorophore would take its chances with the full ambient oxygen concentration. Such a mechanism would be the photochemical equivalent of predator–prey interactions in ecology, where it is often advantageous for the prey to school together or breed in synchrony in order to minimize losses to predation (Wilson, 1975).

Experiment

Theory is all well and good, but empirically how does the photodestruction quantum yield depend on intensity? White and Stryer (1987) tested R-phycoerythrin in a flow system and found that the rate of photodestruction was indeed directly proportional to laser power so that the quantum yield was constant. Unfortunately, the range of intensities tested only went up to about 10^{20} photons $\cdot$ $\text{cm}^{-2}\cdot\text{s}^{-1}$, so that they were still 3 orders of magnitude below saturation of the phycoerythrin. Peck and colleagues (1989) examined B-phycoerythrin and found that photodestruction saturated with increasing input intensity in just the same way as fluorescence emission, so that the photodestruction quantum yield was roughly constant even when the phycobiliproteins were heavily driven into saturation. However, there was some indirect evidence that simpler fluorophores may undergo a nonlinear acceleration of bleaching under such conditions. White *et al.* (1987) reported that bleaching by their scanning confocal microscope seemed to be greatest at the plane of focus. Because the plane of focus receives about the same time-averaged photon flux but much higher peak intensities than out-of-focus planes do, preferential bleaching at the plane of focus would imply that a given number of photons are more injurious when they are bunched, that is, that the photodestruction quantum yield increases at high intensities. Obviously, further testing of this possibility and improvement in photon collection efficiency will be of great importance in confocal microscopy.

A number of workers have reported that damage to biological structures (as distinct from bleaching of the fluorophore) can sometimes be reduced if the given total number of photons is delivered with high intensities for short times rather than low intensities for long times. An early report of the advantage of pulsed illumination was by Sheetz and Koppel (1979) studying the crosslinkage of spectrin by illumination of fluoresceinated concanavalin A on erythrocyte membranes. Bloom and Webb (1984) found similar results for lysis of XRITC-labeled air-equilibrated erythrocytes, whereas well-deoxygenated cells were much more resistant but lysed after a constant total photon dose regardless of whether delivered quickly or slowly. Recently Vigers and colleagues (1988) showed that increasing the illumination intensity up to about $10^3\,\text{W/cm}^2$ decreased the time required for fluorescein-labeled microtubules to dissolve, as one might expect. Surprisingly, intensities above this threshold actually stabilized the microtubules against dissolution, so that the dissolution time became a linearly *increasing* function of intensity. This paradoxical stabilization at high intensities was attributed to local heating based on the assumption that diffusion of heat was negligible. Because this assumption needs to be checked (see Axelrod, 1977; Bloom and Webb, 1984) and because microtubule stabilization and dissolution are not well-defined molecular events, the local heating hypothesis should be viewed with caution. Bonhoeffer and Staiger (1988) have reported that photodynamic damage to rat hippocampal cells was reduced if the light is delivered at 100 exposures each 200 ms long separated by 30 s dark periods rather than continuously for 20 s. They speculated that intermittent illumination was better because it allowed repair mechanisms to operate during the dark intervals. It should be noted that in all the above biological examples, the illumination intensity was well below that expected to be necessary to reach saturation of excited state dye populations (see also Chapter 38, *this volume*).

STRATEGIES FOR SIGNAL OPTIMIZATION IN THE FACE OF PHOTOBLEACHING

Light Collection Efficiency

The above discussion has shown that to increase signal amplitude and S/N in laser-scanning confocal microscopy, increasing laser power helps only until the onset of saturation, and increasing observation time is limited by photodestruction. What other measures can be tried? Obviously any increase in light-collection efficiency (i.e., higher numerical aperture of the objective), transmission efficiency through the scanner and λ filters, and quantum efficiency of photodetection is extremely valuable. Despite the importance of these factors, newcomers to low-light-level microscopy often use low numerical aperture (NA) objectives, excessively narrow emission bandpass filters, inefficient optical couplings, and photomultipliers of less-than-optimal quantum efficiencies. Nearly all the fluorophores that fluoresce strongly in aqueous solution with visible λs of excitation are characterized by small Stokes shifts, or difference between absorption and emission peak λs. It may then be difficult to find or fabricate filters and dichroic mirrors that efficiently separate the two λ bands. In that case, it would usually be preferable to displace the excitation λ to shorter λs away from the peak of the excitation spectrum, so that the emission filters can accept as much of the entire output as possible. Although the excitation is less efficient, this can be made up by increased laser power as long as the photobleaching is reduced by the same factor. By contrast, if the excitation is at the peak λ and the emission acceptance band is pushed to longer λs that exclude much of the emission spectrum, then emitted photons are wasted, while excess scattered photons are collected. The S/N ratio is thus lowered. This is often a severe problem with rhodamine excited using the 514 nm line of the argon-ion laser.

Spatial Resolution

Another tactic to increase signal is to increase the effective size of the confocal apertures, that is, decrease the spatial resolution. If the illuminating and detecting aperture diameters are doubled, the pixel area quadruples and the volume sampled will increase 8-fold. Assuming the total laser power is increased to maintain the same intensity in photons $\cdot\,\text{cm}^{-1}\cdot\text{s}^{-1}$ and that the fluorophore concentration is uniform in the increased volume (as might be true for an ion indicator distributed in the cytosol), the signal should increase 8-fold, though at the price of degraded spatial resolution.

Protective Agents

As mentioned above, light-induced damage to both the fluorophore and to the biological specimen is often dependent on the presence of molecular oxygen, which reacts with the triplet excited states of many dyes to produce highly reactive singlet oxygen. Reduction of the partial pressure or concentration of oxygen often greatly increases the longevity of both the fluorophore and the specimen. In dead, fixed samples, it has become common to add antioxidants

such as propyl gallate (Giloh and Sedat, 1982), hydroquinone, *p*-phenylenediamine, etc., to the mounting medium. The preservative effects of these agents may go beyond removing oxygen because White and Stryer (1987) found propyl gallate to be more effective than thorough deoxygenation at protecting phycoerythrin *in vitro*. One might speculate that polyphenols like propyl gallate might quench dye triplet states and other free radicals, which could prevent forms of photodegradation other than singlet oxygen formation. Protection of GFP and fluorophores from photobleaching in fixed cells has been discussed recently by Bernas and colleagues (2004).

The problem of protecting living cells from oxygen-dependent photodynamic damage is more difficult. The above antioxidants would not be attractive because they would be expected to have strong pharmacological effects at the high concentrations generally employed on fixed tissue. If the tissue can tolerate hypoxia or anoxia, one would probably prefer to remove O_2 by bubbling the medium with N_2 or Ar rather than using chemical reductants. Biological oxygen-scavenging systems such as submitochondrial particles or glucose oxidase + glucose are often helpful (Bloom and Webb, 1984).

If one cannot reduce the O_2 concentration, the next best tactic may be to use singlet oxygen quenchers. The most attractive here are those already chosen by natural selection, namely carotenoids. Their effectiveness is shown by classic experiments in which carotenoid biosynthesis was blocked by mutation; the resulting mutants were rapidly killed by normal illumination levels at which the wild type thrived (Matthews and Sistrom, 1959). A water-soluble carotenoid would be easier to administer acutely than the usual extremely hydrophobic carotenoids such as carotene itself. The most accessible and promising candidate is crocetin, which is the chromophore that gives saffron its color, and which consists of seven conjugated C = C units with a carboxylate at each end. Crocetin quenches aqueous singlet oxygen with a bimolecular rate constant of $5.5 \times 10^9 M^{-1} \cdot s^{-1}$, which is almost diffusion controlled; of this rate, about 95% represents catalytic quenching and about 5% represents bleaching or consumption of the crocetin (Manitto *et al.*, 1987; somewhat more pessimistic rate constants are reported by Matheson and Rodgers, 1982). Longer-chain carotenoids are supposed to be even more efficient at destroying singlet oxygen without damage to themselves, but have not yet been tested in aqueous media. There is some evidence that 50 μM of either crocetin or etretinate (a synthetic aromatic retinoid) can protect cultured cells (L cells and WI-38 fibroblasts) from hematoporphyrin-induced photodynamic damage (Reyftmann *et al.*, 1986). Other water-soluble agents that might be considered as sacrificial reactants with reactive oxygen metabolites include ascorbate (e.g., Vigers *et al.*, 1988), imidazole, histidine, cysteamine, reduced glutathione (Sheetz and Koppel, 1979), uric acid, and Trolox, a vitamin E analog (Glazer, 1988); these would have the advantage over carotenoids of being colorless and non-fluorescent, but would have to be used in much higher concentrations (probably many millimolar) because their bimolecular reaction rates with oxygen metabolites are not as high and they are consumed by the reaction rather than being catalytic. It should also be remembered that thorough deoxygenation may increase the triplet state lifetime, τ_T and worsen the problem of excited-state saturation.

Fluorophore Concentration

Increasing the concentration of fluorophore molecules will only increase the signal as long as they do not get too close together. When multiple fluorophores are attached within a few nanometers of each other on a macromolecule, they usually begin to quench each other. For example, the relatively high quantum yield for free fluorescein in aqueous solution at pH 7 is reduced to near 0.25 when an average of 5 fluorophores are bound to each IgG antibody (Southwick *et al.*, 1990). Charge–transfer interactions with tryptophanes are yet another mechanism for quenching fluoresceins bound to a protein, for example, anti-fluorescein antibody (Watt and Voss, 1977). Most rhodamines and certain cyanines also show a striking reduction in average quantum yield on conjugation, which appears to arise from dye interactions on the protein surface. Absorption spectra of labeled antibodies clearly show evidence of dimers, and fluorescence excitation spectra demonstrate that these dimers are not fluorescent. The propensity of relatively nonpolar, planar rhodamines to interact with one another is not surprising. Even if the fluorophores do not form ground-state dimers, they can also rapidly transfer energy from one to another until a quencher such as O_2 is encountered. In other words, proximity-induced energy transfer between fluorophores multiplies the efficacy of quenchers. Perhaps fortunately it also shortens the excited-state lifetime, so that a higher intensity of laser excitation can be applied for a given degree of saturation (Hirschfeld, 1976). If such increased intensity is available, much of the emission intensity lost by fluorophore proximity can be regained, but at the cost of increased background signal from Rayleigh and Raman scattering and other non-saturated fluorophores.

Choice of Fluorophore

Perhaps the most drastic alteration is to change to a different fluorophore altogether. Unfortunately, there is not a wide selection of fluorescent physiological indicator probes that respond selectively to a cellular parameter and can be excited at appropriate λs. However, with fluorescent labeling reagents, it is sometimes possible to choose an optimal fluorophore within a defined λ range. A selection of fluorescent labels for confocal microscopy is described below.

FLUORESCENT LABELS FOR ANTIBODIES, OTHER PROTEINS, AND DNA PROBES

Fluorescent Organic Dyes

Certain fluorescent reagents carry reactive groups for covalent attachment to target biomolecules and show minimal spectral sensitivity to environmental changes (Table 16.1). These reagents are primarily used to quantify the presence and distribution of probes and targets. The most well-known dyes of this type are derivatives of fluorescein and rhodamine (e.g., tetramethyl rhodamine, lissamine rhodamine, and sulforhodamine 101). A variety of reactive groups have been incorporated into these dyes permitting coupling of the dyes to different functionalities. Isothiocyanates, succinimidyl esters, and pentafluorophenyl esters couple with amino groups of target molecules, while haloacetamides, maleimides, and vinyl sulfones react with sulfhydryl groups. Dichlorotriazinyl (DCT) groups can couple effectively with both amines and alcohols, depending upon reaction pH and temperature. Reactivity and selectivity of the conjugation reactions can be manipulated by the reactive groups chosen and the conditions of the coupling reaction (e.g., reaction pH, solvent polarity, and temperature).

The cyanine dyes (Mujumdar *et al.*, 1993), the borate–dipyrromethene (BODIPY) complexes (Wories *et al.*, 1985; Kang *et al.*, 1988), and the AlexaFluor dyes (Panchuk–Voloshina

et al., 1999) have been developed to complement the traditional fluorescein and rhodamine reagents. The sensitivity of detecting fluorescent conjugates is determined by the spectral properties of the fluorescent dye (its molar extinction coefficient and fluorescence quantum yield) and the quality of the dye–target conjugate (i.e., its tendency to precipitate and its degree of fluorescence quenching). The cyanine reagents, and later the AlexaFluor dyes, were engineered to have very high water solubility as well as excellent spectral properties. Galbraith and colleagues (1989) and Mujumdar and colleagues (1993) have shown that, at least in the case of cyanine dye labeling agents, appropriate placement of charged sulfonate groups on the fluorophore can reduce dye interactions and increase the brightness of relatively heavily labeled antibodies. Particularly useful in this regard are the indopentamethine–cyanines, CY5 dyes (excitation, 630–650 nm; emission 670 nm) and indotrimethine–cyanines, CY3 dyes (excitation, 530–550 nm; emission 575 nm). Antibodies labeled with these dyes have a brightness comparable to or brighter than fluorescein-labeled antibodies and have little tendency to precipitate from solution even when labeled with as many as 10 dye molecules/antibody (Wessendorf and Brelje, 1992). CY5 is somewhat more photostable than fluorescein, and CY3 is significantly more stable. CY5 can be optimally excited with a red He/Ne laser, whereas CY3 can be excited fairly efficiently with the 514 nm line and marginally well with the 488 nm line of the argon-ion laser. These fluorophores are useful for nucleic acid labeling and have found wide use in *in situ* hybridization and gene expression assays. Fluorescent reagents, structurally related to the cyanines, with a squaric acid group replacing part of the polymethine chain have been described (Oswald *et al.*, 1999). Also, novel polymethine dyes developed by Czerney's group were introduced recently as fluorescent reagents (Czerney *et al.*, 2001). These new fluorescent reagents in combination with fluorescein, the phycobiliproteins, or other fluorophores make it possible to do multi-color fluorescence imaging with laser-scanner microscopes equipped with an argon and a He/Ne laser or with the argon/krypton "white light" laser, which has lines at 488, 568, and 647 nm. Brelje and colleagues (1993) have described the use of the Ar/Kr laser to excite samples stained with fluorescein (488 excitation); Texas Red, Lissamine, or CY3 (568 nm); and CY5 (647). Fluorescent labeling reagents available commercially are described on the following Web sites: http://www.amershambiosciences.com; http://www.probes.com; http://www.dyomics.com; and http://www.mobitec.de.

Phycobiliproteins

Phycobiliproteins (Oi *et al.*, 1982) currently hold the record for the highest extinction coefficients and largest number of photons emitted before bleaching (Q_e/Q_b; Mathies and Stryer, 1986), partly because each macromolecule simply contains a large number of component fluorophores, partly because the proteins have been engineered by natural selection to protect the tetrapyrrole fluorophores from quenching processes (Glazer, 1989; Sun *et al.*, 2003). Suitable optimization of laser power, optics, flow rate, and detection permits the detection of fluorescence pulses from single phycobiliprotein molecules in flowing systems (Peck *et al.*, 1989; see also Nguyen *et al.*, 1987). Phycoerythrin (PE) in combination with fluorescein has been valuable for immunofluorescence determination of cell-surface markers by single laser (488 nm excitation) flow cytometry. This approach can also be useful in confocal microscopy, provided that the emission signal is split into a 530 nm (fluorescein) and a 575 nm component (PE) and two photomultipliers are used for detection. Detection of a third color is possible using another photosynthetic protein, PerCP (Rechtenwald, 1989), or the PE tandem conjugates formed by coupling energy acceptor fluorophores that emit at long λs to PE. PE conjugates with Texas Red or to CY5 (Waggoner *et al.*, 1993) have become popular for cell surface measurements with flow cytometers using a 488 nm laser. Phycobiliproteins have also been coupled with CY7 dyes providing additional choices of fluorescence colors (Gerstner *et al.*, 2002; Roederer *et al.*, 1996; Beavis and Pennline, 1996). The use of phycobiliproteins is likely to prove less useful for intracellular antigens because the size of a PE–antibody conjugate, around 410 kD, restricts penetration into denser regions of fixed cells and tissues. Efforts to develop low-molecular-weight analogs of PE that have similarly large Stokes shifts and excitation λs have not yet been successful, but work in this area continues. If fluorophores with large Stokes shifts could be found for both 488 nm and 633 nm excitation, a two-laser microscope could obtain four-color immunofluorescence images. Other probes are listed in Table 16.1.

DNA Probes

An application of fluorescent labels that has attracted a number of investigators is fluorescence *in situ* hybridization, or FISH (Trask, 1991). Initially, DNA to be used to probe genetic sequences in chromosomes and interphase nuclei was labeled by nick translation using biotin or digoxigenin-tagged deoxynucleotide triphosphates (dNTPs). Fluorescent secondary reagents were applied after hybridization to detect the binding of the DNA probe. The use of dNTPs attached by linker arms to fluorophores to form directly labeled fluorescent DNA probes is replacing methods involving fluorescent secondary reagents. Directly labeled DNA probes are simpler to use, often give less background and provide easier access to multi-color–multi-sequence detection (Ballard and Ward, 1993). However, for detection of short genetic sequences, use of multiple fluorescent secondary reagents may be required for sufficient sensitivity. Directly labeled oligonucleotides provide alternatives when there are numerous copies of the target sequence, as in the case of histone mRNA (Yu *et al.*, 1992). For non-specific, but stable labeling of DNA, the bis-intercalating reagents, TOTO, YOYO, DRAQ5, etc., provide an attractive solution, and the reagents are available in several fluorescent colors (Rye *et al.*, 1992). The anthraquinone derivative, DRAQ5, is membrane permeant, is highly selective for nuclear DNA, and can be used with two-photon excitation from 800 nm to beyond 1000 nm. Studies of living cells with DRAQ5 must be done with care because of its high cytotoxicity (Smith *et al.*, 2000; Errington *et al.*, 2005). Snyder (2003) suggests that some caution may be needed when combining DRAQ5 with other probes. There appears to be decreased uptake of bodipy-labelled compounds in the presence of the nuclear stain, DRAQ5.

Luminescent Nanocrystals

Fluorescent nanocrystals, or quantum dots, exhibit interesting properties for biological labeling reagents. These nanometer-sized inorganic crystalloid structures have broad absorption (and excitation) spectra with molar absorptivities of more than six million at 450 nm. The emission band, determined by particle composition and dimensions, can be very narrow (ca. 25 nm FWHM) with quantum yields approaching unity. Also, quantum dot luminescence is very resistant to photobleaching. Selection of uniformly sized quantum dots gives preparations with very sharp fluorescence bands. The challenge for biological applications is to provide biocompatible surfaces for the nanocrystals that maintain their fluorescence in

TABLE 16.1. Spectroscopic Properties of Selected Probes

Parameter	Probe[a]	Absorption Maximum[b]	Extinction Maximum[c]	Emission Maximum[b]	Quantum Yield	Measurement Conditions	References[d]
Covalent labeling reagents	Fluorescein-amines, sulfhydryl	490	67	520	0.71	pH 7, PBS	Haugland (1983), W, MP
	Tetramethylrhodamine-amines	554	85	573	0.28	pH 7, PBS	Haugland (1983), MP
	X-rhodamine-amines	582	79	601	0.26	pH 7, PBS	W
	Texas Red®-amines	596	85	620	0.51	pH 7, PBS	Titus *et al.* (1982), W, MP
	CY3	554	130	568	0.14[f]	pH 7, PBS	Mujumdar *et al.* (1993)
	CY5	652	200	672	0.18[f]	pH 7, PBS	Mujumdar *et al.* (1993)
	CY7	755	200	778	0.02[f]	pH 7, PBS	Mujumdar *et al.* (1993)
	BODIPY® FL	502	80	510		MeOH	MP
	BODIPY 581/591	581	136	591		MeOH	MP
	BODIPY 630/650	625	101	640		MeOH	MP
	Cascade Blue®	378, 399	26	423		Water	MP
	AlexaFluor® 430	430	15	545		pH 7	MP
	AlexaFluor 488	494	73	517		pH 7	MP
	AlexaFluor 532	530	81	555		pH 7	MP
	AlexaFluor 594	590	92	617		pH 7	MP
	NBD-amine	478	24.6	520–550	0.36/0.21	EtOH/MeOH	Kenner & Aboderin (1971), Allen & Lowe (1973), Bratcher (1979)
	NBD-S-CH2CH2OH	425	12.1	531	0.002	pH 7.5, 10% glycerol	
	Coumarin-phalloidin	387		470		Water	MP
	DY-555	555	100	580			MoBiTec GmbH (http://www.mobitec.com)
	DY-631	637	185	658			MoBiTec GmbH (http://www.mobitec.com)
	Phycoerythrin-R	480–565	1960	578	0.68	pH 7, PBS	Oi *et al.* (1982)
	Allophycocyanine	650	700	660	0.68	pH 7, PBS	Oi *et al.* (1982)
	PerCP	488		680		pH 7, PBS	Rechtenwald (1989)
Nanocrystals	*(quantum dots)*	365 & higher	~6000@400 nm	400–850+		PBS	
Lanthanide chelates	Europium chelate	340	Determined	615	See FN *i*	Water	Paul (2002)
	Terbium chelate	340	by ligand	545	See FN *j*		Paul (2002)
Expressible labels	EBFP	383	31	445	0.25	pH 7, PBS	Patterson *et al.* (2001)
	ECFP	434	26	477	0.40	pH 7, PBS	Patterson *et al.* (2001)
	EGFP	489	55	508	0.60	pH 7, PBS	Patterson *et al.* (2001)
	EYFP	514	84	527	0.61	pH 7, PBS	Patterson *et al.* (2001)
	DsRed	558	72.5	583	0.68	pH 7, PBS	Patterson *et al.* (2001)
DNA–RNA content[e]	Hoechst 33342	340	120	450	0.83	+DNA (excess)	W
	DAPI	350		470		+DNA (excess)	W
	DRAQ5	646	21	681		PBS	Smith, PJ *et al.* (2000)
	Ethidium Bromide	510	3.2	595		+DNA (excess)	Pohl *et al.* (1972)
	Propidium Iodide	536	6.4	623	0.09	+DNA (excess)	W
	Acridine Orange	480		520		+DNA	Kapuscinski *et al.* (1982), Shapiro (1985)
		440–470		650		+RNA	
	Pyronine Y	549–561	67–84	567–574	0.04–0.26	+ds DNA[f]	Darzynkiewicz *et al.* (1987), Kapuscinski & Darzynkriwicz (1987)
		560–562	70–90	565–574	0.05–0.21	+ds RNA[f]	
		497	42	563	Low	+ss RNA	
	Thiazole Orange	453	26	480	0.08	RNA	Lee *et al.* (1986)
	TOTO-1	514	112	533		MeOH	MP, Rye *et al.* (1992)
	YOYO-3	612	115	631		MeOH	MP, Rye *et al.* (1992)
Membrane potential	diO-Cn-(3)	485	149	505	0.05	MeOH	Sims *et al.* (1974), W
	diI-Cn-(5)	646	200	668	0.4	MeOH	Sims *et al.* (1974), W
	diBA-Isopr-(3)	493	130	517	0.03	MeOH	Sims *et al.* (1974), W
	diBA-C4-(5)	590	176	620		EtOH	W
	Rhodamine 123	511	85	534	0.9	EtOH	EK, Kubin & Fletcher (1983)

TABLE 16.1. (*Continued*)

Parameter	Probe[a]	Absorption Maximum[b]	Extinction Maximum[c]	Emission Maximum[b]	Quantum Yield	Measurement Conditions	References[d]
pH	BCECF	505		530		High pH	MP
		460				Low pH	MP
	SNARF-1 (pKa = 7.5)	518–548		587		pH 5.5	MP
		574		636		pH 10.0	MP
	DCDHB	340–360		500–580		High pH	Valet *et al*. (1981), MP
		340–360		420–440		Low pH	
Membrane location and fluidity	Diphenylhexatriene (DPH)	330, 351, 370	77 (351 nm)	430		Hexane	MP
	diI-C18-(3)	546	126	565	0.07	MeOH	W
	DiO	484	149	501		MeOH	MP
	DiA	491	52	613		MeOH	MP
	NBD phosphatidylethanolamine	450	24[g]	530		Lipid	Struck *et al*. (1981)
	Anthroyl stearate	361, 381	8.4, 7.5	446		MeOH	Waggoner & Stryer (1970)
	Pyrene-sulfonamidoalkyls	350	30	380–400			MP
Calcium[h]	Fura 2	335	33	512–518	0.23	Low calcium	Grynkiewicz *et al*. (1985)
		360	27	505–510	0.49	High calcium	
	Indo 1	330	34	390–410	0.56	High calcium	Grynkiewicz *et al*. (1985)
		350	34	482–485	0.38	Low calcium	
	Fluo-3	506	83	526	0.183	High calcium	Minata *et al*. (1989) & Mukkala *et al*. (1993), MP
		506	78	526	0.0051	Low calcium	
O_2 sensor	$Ru[dpp(SO_3Na)_2]_3$	365/450		590	$\tau = 3.7\,\mu s$	No oxygen	Castellano & Lakowicz (1981)
					$\tau = 0.93\,\mu s$	Air	
cAMP	FIERhR	490	70	520, 573	—	pH 7, cAMP	Adams *et al*. (1991)
Enzyme substrates	Rhodamine-di-arg-CBZ	495	—	532	0.09	Hepes pH 7.5	Leytus *et al*. (1983)
	Product of rxn. (rhodamine)	495	67	523	0.91	+15% EtOH	
	Coumarin-glucoside substr.	316	13	395		pH 5.5 + 1% Lubrol	W
	Rxn. product (hydroxy coumarin)	370	17	450		pH10 + 1% Lubrol	W
	Fluorescein digalactosidase product	490	67	520	0.71	pH 7, PBS	MP
	Resorufin galactosidase product	571	58	585		pH 9	MP
	ELF97 phosphatase product	345	Precipitate	530		pH 8	MP

[a] Abbreviations: NBD, 7-nitrobenz-2-oxa-1,3-diazole; DAPI, 4′,6-diamidino-2-phenylindole; DCDHB, dicyano-dihydroxybenzene.
[b] Measured in nanometers.
[c] Multiply value listed by 1000 to get liters/mol·cm.
[d] EK, Eastman Kodak Chemical Catalog; MP, Molecular Probes, Inc catalog; W, Waggoner laboratory determination.
[e] See Table III in Arndt-Jovin & Jovin (1989) for additional DNA content probes.
[f] Base-pair dependent.
[g] Value for NBD-ethanolamine in MeOH which has an abs.max at 470 nm and an emission max at 550 nm [Barak & Yocum (1981)].
[h] See Tsien (1989) for additional details and other ion indicators.
[i] See corporate Web sites: Quanturm Dot Corp. (www.qdots.com), Evident Technologies (www.evidenttech.com), BioCrystal, Ltd. (www.biocrystal.com) and Crystalplex Corp. (www.crystalplex.com).
[j] Time resolved detection. Extinction times quantum yield approx. 2100.

aqueous media. Promising results have been obtained using quantum dots (Jaiswal *et al.*, 2003; Hoshino *et al.*, 2004; Voura *et al.*, 2004). However, there is ample opportunity for significant improvements before these reagents can be used routinely for fluorescent labeling. Their relatively large size and high mass limit their use in applications requiring high diffusional mobility.

Fluorescent Lanthanide Chelates

Lanthanide chelates are another group of fluorescent reagents with special spectral properties. These reagents have microsecond fluorescence lifetimes that are readily distinguished from typical nanosecond autofluorescence background (Soini *et al.*, 1988; Seveus *et al.*, 1994; Vereb *et al.*, 1998). Temporal separation of probe fluorescence from background signal can give a very high S/N and highly sensitive probe detection even though the brightness of these reagents is only modest. The main advantage of these compounds is that, as their fluorescent properties are dependent on electron energy levels in an atom rather than those of a molecule, they are very resistant to photodamage (and perhaps also to phototoxicity). On the other hand, it is possible that the excitation light may break the bond with the chelator causing the "dye atom" to become a non-specific stain.

The current versions of these reagents require enhanced antennary ligands for more efficient lanthanide excitation and improved biological stability and compatibility. On the other hand, the long decay times give rise to problems when they are used in scanning microscopes. When the decay time is equal to the pixel dwell time,

each molecule can be excited no more than one time and signal levels are very low. As a result, these dyes will probably only be used with widefield imaging where the exposure time seen by each molecule is long compared to its fluorescent lifetime and discrimination from the fast decay of the autofluorescence is still useful.

FLUORESCENT INDICATORS FOR DYNAMIC INTRACELLULAR PARAMETERS

Membrane Potentials

The use of confocal microscopy to measure dynamic properties of living cells such as membrane potentials (Gross and Loew, 1989) or ion concentrations (Tsien, 1988, 1989a,b) deserves some special comment. Preliminary attempts to use fast-responding, non-redistributive voltage-sensitive dyes in neuronal tissues were unsuccessful (Fine *et al.*, 1988); the dye could be seen, but the S/N was inadequate to observe voltage-dependent changes, which would have been at most only a few percent of the resting intensity. Lasers are inherently noisy light sources; even with optical negative feedback, their fluctuations are greater than the stabilized tungsten filament lamps conventionally used to see the small changes in fluorescent output that characterize fast voltage-sensitive dyes (Cohen and Lesher, 1986). "Slow" redistributive dyes, which accumulate in cells according to the Nernst equilibrium (Ehrenberg *et al.*, 1988), would seem to be more suitable for present-day confocal microscopes because their signals are much bigger and the slowness of their response (seconds to minutes) is actually a better match to the rather slow scan times of the current instrumentation. Confocal optical sectioning should work well using such accumulative dyes because in principle one could directly compare the internal concentrations of dye accumulated without having to correct for the greater path length of a thicker cell or for extracellular dye above and below the plane of focus. Freely diffusing anionic oxonol dyes have been paired with dyes anchored at the cell surface permitting fast ratiometric detection of membrane potential changes in single cells by fluorescence resonance energy transfer (Gonzalez and Tsien, 1995, 1997; Gonzalez and Maher, 2002) (see also Figure 8.45, *this volume*).

Ion Concentrations

Wavelength Ratioing

Some indicators of ion concentrations respond not just with changes in fluorescence amplitude but also with λ shifts of the excitation or emission spectrum or both. Such shifts permit ratioing between signals obtained at two or more λs (Tsien, 1989a,b). Ratioing is highly valuable because it cancels out differences in dye concentration and path length as well as fluctuations in overall illumination intensity (Tsien and Poenie, 1986; Bright *et al.*, 1987). Emission ratioing is the most valuable because, with a single excitation λ, the emission can be passed through a dichroic mirror to split it into two bands that can be monitored absolutely simultaneously. Such ratioing would give the best possible cancellation of laser noise or specimen movement. Emission ratioing is particularly easy to do with a laser-scanning system, because one can simply add a dichroic mirror and an extra photodetector after the scanning system. Whereas geometrical registration of all the corresponding pixels in two separate low-light-level video cameras is quite difficult (Jericevic *et al.*, 1989), the registration problem is trivial in a laser-scanning system assuming that the deflection is achromatic, which it must be in order to get excitation and even one emission in register. Disk-scanning confocal microscopes use charge-coupled device (CCD) or electron multiplying CCD (EM-CCD) cameras as detectors and often lack this elegant compatibility with emission ratio scanning.

Excitation ratioing of images requires sequential illumination with the two excitation λs. Intensity fluctuations of the source and movement of the specimen are canceled out only if they are much slower than the rate of alternation. Excitation ratioing is most applicable to tandem-scanning systems where conventional systems for alternating two grating monochromators or interference filters could be used. Alternating between two laser lines is more convenient now that acousto-optical deflectors are common, but it is still less flexible in choice of λ pairs.

pH Indicators

A number of ratiometric pH indicators were reviewed by Tsien (1989b) and more recently by Yip and Kurtz (2002). The most popular excitation-ratioing indicator is probably the modified fluorescein, BCECF, whose pH-sensitive and insensitive λs are around 490 nm and 439 nm, respectively. Several emission-shifting probes, 3,6-dihydroxyphthalonitrile (also known as 2,3-dicyanohydroquinone; Kurtz and Balaban, 1985; Kurtz and Emmons, 1993), and various naphthofluorescein derivatives (SNAFs and SNARFs; Haugland, 1989) are also available.

Ca^{2+} Indicators

Three currently available Ca^{2+} indicators have different sets of advantages and disadvantages for confocal microscopy (Tsien, 1988, 1989a,b). Fura-2, the dye most used in conventional microscopic imaging, shows a good excitation shift with Ca^{2+}, typically ratioed between 340 to 350 nm and 380 to 385 nm, but hardly any emission shift, so it would be most effectively used with a UV-enhanced disk-scanning instrument. Considerable re-engineering would be necessary for those early designs of tandem-scanning confocal microscope designed mainly for reflectance rather than fluorescence. The beam-splitting pellicles used are inefficient because they are partially reflective but not dichroic; also, they are sometimes made from UV-blocking material in which the excitation has to pass through the pellicle whereas the emission would have to reflect off the pellicle. Even if the pellicle were replaced by a dichroic, this choice of beam geometry is unfortunate, as it is much easier to make good broadband dichroics in which the shorter λ reflects and the longer λ transmits than vice versa. Disk systems in which the same area of the disk is used for both source and detector may be more flexible (see Chapter 10, *this volume*).

Indo-1, the dye most used in laser flow cytometry for [Ca^{++}] determination, shows a fine emission shift from 485 to 405 nm with increasing Ca^{2+} and is preferred for ratiometric laser scanning. However, either a UV laser (e.g., a high-power argon-ion or krypton-ion system) or a titanium–sapphire two-photon system is required for excitation in the 350 to 365 nm region. Also, Indo-1 fluorescence has λs similar to those of reduced pyridine nucleotides, so autofluorescence could be a problem, and Indo-1 also bleaches much more quickly than Fura-2.

Fluo-3 and its less-tested rhodamine analogs are the only Ca^{2+} indicators currently available with visible λs suitable for low-power visible lasers (Minta *et al.*, 1989; Kao *et al.*, 1989). Therefore, it has been the first to be exploited in confocal microscopy (e.g., Hernandez-Cruz *et al.*, 1989), even though it lacks either an

excitation or emission shift and is restricted to simple intensity measurements that are relatively difficult to calibrate in terms of absolute $[Ca^{2+}]_i$ units.

Of course, the ideal would be an indicator excitable at 488 nm with a large emission shift, high quantum efficiency, and strong resistance to bleaching, but this goal is a difficult challenge in molecular engineering. In general, strong fluorescence in aqueous media is much easier to obtain using shorter excitation λs because fluorescence demands planarity and molecular rigidity, which is obviously easier to achieve in small molecules that absorb short λs than in the larger molecules with longer chromophores. Most of the known chromophores that combine large size, long λs, and rigidity are essentially insoluble in water. Even if solubilizing groups are added on the periphery, the huge expanse of hydrophobic surface still promotes the formation of non-fluorescent aggregates. Finally, the quantum mechanics of absorption and fluorescence predict that the intrinsic radiative lifetime of a chromophore is proportional to the cube of the λ if other factors remain constant (Strickler and Berg, 1962). Short radiative lifetimes mean that fluorescence emission competes more successfully with nonproductive forms of deactivation and, therefore, correlates with high quantum yields of fluorescence.

Oxygen Sensor

Much effort has been spent developing ruthenium chelates as luminescent reagents. Common ligands for the central ruthenium ion include substituted bipyridines and 1,10-phenanthrolines. Currently, the most promising applications for these complexes are for monitoring the oxygen tension of solutions (Li *et al.*, 1997; Castellano and Lakowicz, 1998; Ji *et al.*, 2002). As with the lanthanide complexes, the modest excitation efficiencies are dependent on energy transfer from the ligands to the metal ion. The emission spectra are relatively weak and broad. However, time-resolved detection of the long-lived ruthenium fluorescence yields excellent S/N even from these low intensities. The presence of oxygen, even at the levels found in air, decreases the fluorescence lifetimes of ruthenium chelates by a factor of 4, a factor that should make them suitable for fluorescence lifetime imaging (FLIM; see Chapter 27, *this volume*), now that the equipment is commercially available. Improved ligands with enhanced absorbance at visible wavelengths, more efficient energy transfer to the metal, and better biocompatibility are needed before these reagents find broader applications.

cAMP Indicators

The important intracellular messenger cAMP (cyclic adenosine 3,5-monophosphate) can now be imaged with a fluorescent indicator made from cAMP-dependent protein kinase labeled on its C and R subunits with fluorescein and tetramethylrhodamine respectively (Adams *et al.*, 1991). In the holoenzyme complex, the fluorescein and rhodamine are close enough for moderately efficient fluorescence resonance energy transfer, so that excitation of the fluorescein with blue-green light gives a significant amount of orange emission from the rhodamine. Binding of cAMP dissociates the subunits and eliminates energy transfer, increasing the emission of green light directly from the fluorescein and decreasing the amplitude in the rhodamine band. This change in emission ratio and the λs employed are ideal for dual-channel detection by confocal microscopy (Bacskai *et al.*, 1993). The strategy of labeling an important endogenous sensor protein gives both advantages and potential problems. Because careful derivatization of the kinase does not change its cAMP affinity and phosphorylating activity, the indicator is inherently tuned to the physiologically relevant concentration range (a few nanomoles to a few examoles), and molecules of cAMP that bind to the indicator can still have a biological effect. An indicator that was not a physiological effector molecule would have a greater tendency to competitively inhibit or buffer the pathway under study. Furthermore, after elevation of cAMP, the interesting trafficking of the R and C subunits can be separately observed by standard dual-label imaging (e.g. Harootunian *et al.*, 1993). However, scrambling of subunits with unlabeled endogenous kinase is a potential problem, so far rarely serious (for discussion of this point and a more extensive review of the entire technique, see Adams *et al.*, 1993).

Fatty Acid Indicator

Fatty acids are of considerable importance in nutrition, membrane structure, protein modification, eicosanoid formation, and modulation of cell signaling. Recently a group led by Alan Kleinfeld has developed an emission-ratioing fluorescent probe for free fatty acid levels (Richieri *et al.*, 1992) by labeling recombinant intestinal fatty-acid-binding protein with acrylodan, an environmentally sensitive fluorophore. The acrylodan reacts with surprising specificity for Lys27 of the protein and probably resides in the fatty-acid binding pocket. Binding of fatty acids shifts the emission peak from 432 nm to 505 nm, probably by displacing the acrylodan into an aqueous environment. The 505 nm/432 nm ratio thereby increases by up to 25-fold, which would be an ideal signal for confocal microscopy if the necessary excitation at 386 nm or 400 nm were available. The labeled protein (dubbed ADIFAB) binds all common long-chain fatty acids with approximately micromolar dissociation constants. In a cuvet, ADIFAB can detect free fatty acid concentrations as low as a few nanomolar. It has already proven highly useful in measuring the release of free fatty acids from stimulated rat basophilic leukemia (RBL) cells (Richieri *et al.*, 1992) and the binding constants of fatty acids to albumin (Richieri *et al.*, 1993) and to cells (Anel *et al.*, 1993).

Other Forms of Ratioing

Because ratioing is so desirable for quantitative measurements, but appropriate λ shifts are often unavailable, several alternatives to λ ratioing have been proposed. The easiest is simply to ratio poststimulus image intensities against a prestimulus image. An example is shown by Smith and Augustine (1988). This method has the advantage of minimal hardware requirements and high time resolution, though it only cancels out variations in dye loading and path length, not shape change or dye bleaching, and by itself cannot yield an absolute calibration of the analyte, for example, $[Ca^{2+}]_i$. Another approach would be to link the fluorescent indicator covalently to a separate reference fluorophore. This approach would ideally generate a composite molecule in which the ratio of the indicator fluorescence to the reference fluorescence would signal the analyte concentration. Potential disadvantages would be the requirement for significant skill in organic synthesis, the likelihood that the conjugate would be too large for loading by ester hydrolysis, and the possibility that the two fluorophores would bleach at different rates, so that the operation of ratioing would fail to correct for bleaching. Yet a third mode of ratioing could be based on temporal dissection of excited-state lifetimes, as first shown for quin-2 by Wages and colleagues (1987). If the free and bound forms of the indicator have sufficiently different fluorescence lifetimes, their relative contributions to the (ideally) biexponential decay might be separated by nanosecond or high frequency mod-

ulation techniques (see Chapter 27, *this volume*). However, even when the instrumentation challenge of combining lifetime kinetics with imaging has been solved, the problem remains that probes like fura-2 and Indo-1, which are fairly strongly fluorescent both when free and when bound to Ca^{2+}, have almost the same lifetimes in those two states. For example, fura-2 with and without Ca^{2+} has lifetimes of 1.8 ns and 1.3 ns, respectively, at 25°C; for Indo-1 the corresponding numbers are 1.7 ns and 1.3 ns at 20°C (Wages *et al.*, 1987). In order to have a significant difference in lifetimes between Ca^{2+}-bound and free indicator, as in quin-2 (10.1 ns and 1.3 ns, respectively, at 25°C), one of the species has to be much more dimly fluorescent than the other. As a result, the weaker and faster component will be hard to measure accurately and to distinguish from autofluorescence background.

Ratiometric measurements can also be applied to other parameters such as probe polarization and local viscosity (Tinoco *et al.*, 1987; Axelrod, 1989; Dix and Verkman, 1989), proximity between macromolecules by fluorescence energy transfer (Uster and Pagano, 1986; Herman, 1989), and even water permeability (Kuwahara and Verkman, 1988; Kuwahara *et al.*, 1988).

GENETICALLY EXPRESSED INTRACELLULAR FLUORESCENT INDICATORS

Green Fluorescent Protein

Fluorescent proteins from jellyfish and corals have revolutionized biological optical microscopy because they provide genetic encoding of strong visible fluorescence of a wide range of colors. Entire books (Chalfie and Kain, 1998; Sullivan and Kay, 1999; Hicks, 2002) have been devoted to many aspects of the prototypical fluorescent protein, the green fluorescent protein (GFP) from the jellyfish *Aequorea victoria*. A shorter, relatively self-contained introduction to GFP may be found in Tsien (1998). Other general reviews on applications of GFP and other members of the fluorescent protein superfamily include (Cubitt *et al.*, 1995, 1999; Hassler, 1995; Niswender *et al.*, 1995; Rizzuto *et al.*, 1995; Stearns, 1995; Kahana and Silver, 1996; Misteli and Spector, 1997; Patterson *et al.*, 1997; Tsien and Miyawaki, 1998; Ellenberg *et al.*, 1999; Heim, 1999; Lippincott-Schwartz *et al.*, 1999; Phillips, 1999; Piston *et al.*, 1999; Chamberlain and Hahn, 2000; Miyawaki and Tsien, 2000; Sacchetti *et al.*, 2000; Zaccolo and Pozzan, 2000; Zacharias *et al.*, 2000; Blab *et al.*, 2001; Chiesa *et al.*, 2001; Harms *et al.*, 2001; Lippincott-Schwartz *et al.*, 2001; Patterson *et al.*, 2001; Reits and Neefjes, 2001; Wahlfors *et al.*, 2001; Labas *et al.*, 2002; Matz *et al.*, 2002; Miyawaki, 2002; van Roessel and Brand, 2002; Zacharias, 2002; Zhang *et al.*, 2002; Zimmer, 2002; Choy *et al.*, 2003; Ehrhardt, 2003; Hadjantonakis *et al.*, 2003; Lippincott-Schwartz and Patterson, 2003; Lippincott-Schwartz *et al.*, 2003; March *et al.*, 2003; Meyer and Teruel, 2003; Miyawaki, 2003; Tsien, 2003; Viallet and Vo-Dinh, 2003; Weijer, 2003; Verkhusha and Lukyanov, 2004). Space does not permit listing the huge number of reviews and primary papers describing more specialized uses of fluorescent proteins.

Ligand-Binding Modules

Genetic manipulations have also been used to incorporate into cells expressible modules that bind fluorescent ligands. One type of module contains a tetracysteine motif, which binds biarsenical ligands (Griffin *et al.*, 1998; Adams *et al.*, 2002; Nakanishi *et al.*, 2004). These small, membrane-permeant ligands bind with high affinity and specificity to the four sulfhydryls arranged in an alpha helix domain. Biarsenical fluorescein (FlAsH), tetramethyl rhodamine (TrAsH), and a few additional dyes have been reported. In a different approach, cells transfected with the sequence encoding a single-chain antibody (scFv) expressed a module that tightly bound cell-permeant hapten–fluorophore conjugates (Farinas and Verkman, 1999). Incorporation of several scFvs would enable multiple ligands to be detected simultaneously. Like the expressible GFPs, these modules can be directed to specific intracellular compartments by including the appropriate localization sequences.

Ion Indicators

Mutants of GFP have been identified that show pH-dependent fluorescence properties (Kneen *et al.*, 1998; Llopis *et al.*, 1998). Reversible absorbance and fluorescence emission changes were observed with apparent pKa values ranging from 4.8 to 7.1. Combining the GFP sequences with specific targeting signals permitted the acidification of specific organelles to be followed noninvasively. Genetically encoded Ca^{2+} indicators, dubbed "chameleons," utilize fluorescence resonance energy transfer (FRET) between different emitting GFPs attached to calmodulin and a calmodulin-binding peptide, M13 (Miyawaki *et al.*, 1997, 1999). Binding of Ca^{2+} to calmodulin increases the interaction between the GFPs. Optimization of the relative orientation of the two GFPs in the chimeras has expanded the dynamic range of Ca^{2+} detection (Nagai *et al.*, 2001, 2004).

FUTURE DEVELOPMENTS

Speculation on future directions in fluorophore designs is difficult because the small number of laboratories working on fluorophore chemistry makes progress a much noisier function of time than advances in instrumentation or computers. One major advance seen since publication of the previous edition of this book is a recognition of the optimal characteristics for fluorescent reagents used in biology. A thought prompted by preparation of this review is that, for present purposes, the excited triplet state of the fluorophore is a major villain without any redeeming virtues. It is responsible for a pernicious form of output saturation, for singlet oxygen production, and for nearly all covalent photochemistry such as bleaching. Similar problems have been encountered in laser dyes; a proposed solution (Liphardt *et al.*, 1982, 1983; Schäfer, 1983) is to attach triplet-state quenchers to each fluorophore. Such a construction is reminiscent of the way that evolution has assembled photosynthetic complexes and may be an area where biology can repay its debt to synthetic chemistry. Little progress has been reported in this area during the two decades since these approaches were proposed, but the potential gains from triplet-state relaxation maintain this as an attractive area for study. The development of fluorescent inorganic nanocrystals and chelates may provide the needed photostable biological tagging reagents, however.

Another area ripe for development is signal amplification schemes for detecting low copy numbers of cell receptors and genetic sequences. Use of enzymes that produce fluorescent precipitates in a localized area offers promise (Haugland, 1989); again reported progress is limited.

Finally, there is always need for additional sensitivity. Time-resolved fluorescence detection, where the fluorescence signal is collected against a dark background after pulse excitation, offers a method to circumvent autofluorescence and Raman light scat-

tering that is becoming much more widely available (Lakowicz *et al.*, 1983; Marriott *et al.*, 1991; Chapters 27 and 31, *this volume*). This approach is now realized with sophisticated excitation/detection components and will work with any fluorophore with an excited state lifetime in the nanosecond time range. Quantum dots, with fluorescence lifetimes in the range of 20 ns, may prove particularly useful, but their early-stage development as biological labeling reagents has not provided sufficient incentives for the required detection system modifications. Another ingenious approach would involve excitation of an extended lifetime fluorophore with a scanning laser followed by detection of the signal with an array detector, such as a cooled EM-CCD camera, instead of a single photomultiplier tube. The signal could be integrated on the cleared pixels of the CCD chip, even milliseconds after the excitation beam has passed the corresponding region of the sample. The extended lifetime labels could be lanthanide complexes with millisecond lifetimes that have been developed as protein-labeling reagents by Hemmila and others (Soini *et al.*, 1988; Mukkala, 1993). In situations with heavy autofluorescence, the lanthanide complex labels have demonstrated sensitivity over fluorescein labels by factors of hundreds (Seveus *et al.*, 1994). Phosphor particles developed by Beverloo and colleagues (1992) could be used in a similar fashion. Surface chemistries used to improve the biocompatibility of quantum dots may also be effective in enhancing the fluorescence properties of these phosphors in biological applications. Chemistry will continue to play a major role in furthering the power of confocal microscopy.

ACKNOWLEDGMENTS

We thank Profs. Richard Mathies and Alex Glazer for helpful discussions and criticisms of the manuscript and permission to cite their unpublished data.

REFERENCES

Adams, S.R., Campbell, R.E., Gross, L.A., Martin, B.R., Walkup, G.K., Yao, Y., Llopis, J., and Tsien R.Y., 2002, New biarsenical ligands and tetracysteine motifs for protein labeling in vitro and in vivo: synthesis and biological applications, *J. Am. Chem. Soc*. 124:6063–6076.

Adams, S.R., Harootunian, A.T., Buechler, Y.J., Taylor, S.S., and Tsien, R.Y., 1991, Fluorescence ratio imaging of cyclic AMP in single cells, *Nature* 349:694–697.

Adams, S.R., and Tsien, R.Y., 1993, Controlling cell chemistry with caged compounds, *Annu. Rev. Physiol*. 55:755–784.

Anel, A., Richieri, G.V., and Kleinfeld, A.M., 1993, Membrane partition of fatty acids and inhibition of T cell function, *Biochemistry* 32:530–536.

Axelrod, D., 1977, Cell surface heating during fluorescence photobleaching recovery experiments, *Biophys. J*. 18:129–131.

Axelrod, D., 1989, Fluorescence polarization microscopy, *Methods Cell Biol*. 30:333–352.

Bacskai, B.J., Hochner, B., Mahaut-Smith, M., Adams, S.R., Kaang, B.-K., Kandel, E.R., and Tsien, R.Y., 1993, Spatially resolved dynamics of cAMP and protein kinase A subunits in Aplysia sensory neurons, *Science* 260:222–226.

Bailey, E.A. Jr., and Rollefson, G.K., 1953, The determination of the fluorescence lifetimes of dissolved substances by a phase shift method, *J. Chem. Phys*. 21:1315–1322.

Ballard, S.G., and Ward, D.C., 1993, Fluorescence in situ hybridization using digital imaging microscopy, *J. Histochem. Cytochem*. 12:1755–1759.

Beavis, A.J., and Pennline, K.J., 1996, Allo-7: a new fluorescent tandem dye for use in flow cytometry, *Cytometry* 24:390–395.

Bernas, T., Zarebski, M., Cook, R.R., and Dobrucki, J.W., 2004, Minimizing photobleaching during confocal microscopy of fluorescent probes bound to chromatin: Role of anoxia and photon flux, *J. Microsc*. 5:281–296.

Beverloo, H.B., van Schadewijk, A., Bonnet, J., van der Geest, R., Runia, R., Verwoerd, N.P., Vrolijk, J., Ploem, J.S., and Tanke, H.J., 1992, Preparation and microscopic visualization of multicolor luminescent immunophsphors, *Cytometry* 13:561070.

Blab, G.A., Lommerse, P.H.M., Cognet, L., Harms, G.S., and Schmidt, T., 2001, Two-photon excitation action cross-sections of the autofluorescent proteins, *Chem. Phys. Lett*. 350:71–77.

Bloom, J.A., and Webb, W.W., 1984, Photodamage to intact erythrocyte membranes at high laser intensities: methods of assay and suppression, *J. Histochem. Cytochem*. 32:608–616.

Bonhoeffer, T., and Staiger, V., 1988, Optical recording with single cell resolution from monolayered slice cultures of rat hippocampus, *Neurosci. Lett*. 92:259–264.

Brelje, T.C., Wessendorf, M.W., and Sorenson, R.L., 1993, Multicolor laser scanning confocal immunofluorescence microscopy: practical applications and limitations. In: *Methods in Cell Biology 38: Cell Biological Applications of Confocal Microscopy* (B. Matsumoto, ed.), Academic Press, San Diego, California.

Bright, G.R., Fisher, G.W., Rogowska, J., and Taylor, D.L., 1987, Fluorescence ratio imaging microscopy: Temporal and spatial measurements of cytoplasmic pH, *J. Cell Biol*. 104:1019–1033.

Castellano, F.N., and Lakowicz, J.R., 1998, A water-soluble luminescence oxygen sensor, *Photochem. Photobiol*. 67:179–183.

Chalfie, M., and Kain, S., 1998, *Green Fluorescent Protein: Properties, Applications, and Protocols*, Wiley-Liss, New York.

Chalfie, M., Tu, Y., Euskirchen, G., Ward, W.W., and Prasher, D.C., 1994, Green fluorescent protein as a marker for green expression, *Science* 263:802–805.

Chamberlain, C., and Hahn, K.M., 2000, Watching proteins in the wild: fluorescence methods to study protein dynamics in living cells, *Traffic* 1:755–762.

Chen, R.F., and Scott, C.H., 1985, Atlas of fluorescence spectra and lifetimes of dyes attached to protein, *Analyt. Lett*. 18:393–421.

Chiesa, A., Rapizzi, E., Tosello, V., Pinton, P., de Virgilio, M., Fogarty, K.E., and Rizzuto, R., 2001, Recombinant aequorin and green fluorescent protein as valuable tools in the study of cell signaling, *Biochem. J*. 355:1–12.

Choy, G., Choyke, P., and Libutti, S.K., 2003, Current advances in molecular imaging: noninvasive in vivo bioluminescent and fluorescent optical imaging in cancer research, *Mol. Imaging* 2:303–312.

Cohen, L.B., and Lesher, S., 1986, Optical monitoring of membrane potential: Methods of multisite optical measurement, In: *Optical Methods in Cell Physiology* (P. De Weer, B.M. Salzberg, eds.), John Wiley and Sons, New York, pp. 71–99.

Cubitt, A.B., Heim, R., Adams, S.R., Boyd, A.E., Gross, L.A., and Tsien, R.Y., 1995, Understanding, using and improving green fluorescent protein, *Trends Biochem. Sci*. 20:448–455.

Cubitt, A.B., Woollenweber, L.A., and Heim, R., 1999, Understanding structure-function relationships in the Aequorea victoria green fluorescent protein, *Methods Cell Biol*. 58:19–30.

Czerney, P., Lehmann, F., Wenzel, M., Buschmann, V., Dietrich, A., and Mohr, G.J., 2001, Tailor-made dyes for fluorescence correlation spectroscopy (FCS), *Biol. Chem*. 382:495–498.

Dix, J.A., and Verkman, A.S., 1989, Spatially resolved anisotropy images of fluorescent probes incorporated into living cells, *Biophys. J*. 55:189a.

Ehrenberg, B., Montana, V., Wei, M.D., Wuskell, J.P., and Loew, L.M., 1988, Membrane potentials can be determined in individual cells from the Nernstian distribution of cationic dyes, *Biophys. J*. 53:785–794.

Ehrhardt, D., 2003, GFP technology for live cell imaging, *Curr. Opin. Plant Biol*. 6:622–628.

Ellenberg, J., Lippincott-Schwartz, J., and Presley, J.F., 1999, Dual-colour imaging with GFP variants, *Trends Cell Biol*. 9:52–56.

Errington, R.J., Ameer-Beg, S.M., Vojnovic, B., Patterson, L.H., Zloh, M., Smith, P.J., 2005, Advanced microscopy solutions for monitoring the kinetics and dynamics of drug-DNA targeting in living cells, *Adv. Drug Deliv. Rev.* 57(1):153–167.

Farinas, J., and Verkman, A.S., 1999, Receptor-mediated targeting of fluorescent probes in living cells, *J Biol. Chem.* 274:7603–7606.

Fine, A., Amos, W.B., Durbin, R.M., and McNaughton, P.A., 1988, Confocal microscopy: Applications in neurobiology, *Trends Neurosci*. 11:346–351.

Galbraith, W., Ernst, L.A., Taylor, D.L., and Waggoner, A.S., 1989, Multiparameter fluorescence and the selection of optimal filter sets: Mathematics and computer program, *Proc. Soc. Photo. Opt. Instrum. Eng*. 1063:74–122.

Gandin, E., Lion, Y., and Van de Vorst, A., 1983, Quantum yields of singlet oxygen production by xanthene derivatives, *Photochem. Photobiol*. 37:271–278.

Gerstner, A.O., Lenz, D., Laffers, W., Hoffman, R.A., Steinbrecher, M., Bootz, F., and Tarnok, A., 2002, Near-infrared dyes for six-color immunophenotyping by laser scanning cytometry, *Cytometry* 48:115–123.

Giloh, H., and Sedat, J.W., 1982, Fluorescence microscopy: Reduced photobleaching of rhodamine and fluorescein protein conjugates by *n*-propyl gallate, *Science* 217:1252–1255.

Glazer, A.N., 1988, Fluorescence-based assay for reactive oxygen species: A protective role for creatinine, *FASEB J.* 2:2487–2491.

Glazer, A.N., 1989, Light guides. Directional energy transfer in a photosynthetic antenna, *J. Biol. Chem.* 264:1–4.

González, J.E., and Maher, M.P., 2002, Cellular fluorescent indicators and voltage/ion probe reader (VIPR$^{(tm)}$): Tools for ion channel and receptor drug discovery, *Receptors Channels* 8:283–295.

Gonzalez, J.E., and Tsien, R.Y., 1995, Voltage sensing by fluorescence resonance energy transfer in single cells, *Biophys. J*. 69:1272–1280.

Gonzalez, J.E., and Tsien, R.Y., 1997, Improved indicators of cell membrane potential that use fluorescence resonance energy transfer, *Chem. Biol*. 4:269–277.

Griffin, B.A., Adams, S.R., and Tsien, R.Y., 1998, Specific covalent labeling of recombinant protein molecules inside live cells, *Science* 281:269–272.

Gross, D., and Loew, L.M., 1989, Fluorescent indicators of membrane potential: Microspectrofluorometry and imaging, *Methods Cell Biol*. 30:193–218.

Hadjantonakis, A.K., Dickinson, M.E., Fraser, S.E., and Papaioannou, V.E., 2003, Technicolour transgenics: Imaging tools for functional genomics in the mouse, *Nat. Rev. Genet*. 4:613–625.

Harms, G.S., Cognet, L., Lommerse, P.H., Blab, G.A., and Schmidt, T., 2001, Autofluorescent proteins in single-molecule research: Applications to live cell imaging microscopy, *Biophys. J*. 80:2396–2408.

Harootunian, A.T., Adams, S.R., Wen, W., Meinkoth, J.L., Taylor, S.S., and Tsien, R.Y., 1993, Movement of the free catalytic subunit of cAMP dependent protein kinase into and out of the nucleus can be explained by diffusion, *Mol. Biol. Cell* 4:993–1002.

Hasan, M.T., Friedrich, R.W., Euler, T., Larkum, M.E., Giese, G., Both, M., Duebel, J., Waters, J., Bujard, H., Griesbeck, O., Tsien, R.Y., Nagai, T., Miyawaki, A., and Denk, W., 2004, Functional fluorescent Ca^{2+} indicator proteins in transgenic mice under TET control, *PLoS Biol*. 2:763–775.

Hassler, S., 1995, Green fluorescent protein — the next generation, *Bio/Technology* 13:103.

Haugland, R.P., 1989, *Molecular Probes: Handbook of Fluorescent Probes and Research Chemicals*, Molecular Probes Inc., Eugene, Oregon, pp. 86–94.

Heim, R., 1999, Green fluorescent protein forms for energy transfer, *Methods Enzymol*. 302:408–423.

Hernandez-Cruz, A., Sala, F., and Adams, P.R., 1989, Subcellular dynamics of $[Ca^{2+}]_i$ monitored with laser scanned confocal microscopy in a single voltage-clamped vertebrate neuron, *Biophys. J.* 55:216a.

Herman, B., 1989, Resonance energy transfer microscopy, *Methods Cell Biol*. 30:219–243.

Hicks, B.W., 2002, *Green Fluorescent Protein: Applications and Protocols*, Humana Press, Totowa, New Jersey.

Hirschfeld, T., 1976, Quantum efficiency independence of the time integrated emission from a fluorescent molecule, *Appl. Opt*. 15:3135–3139.

Hoshino, A., Hanaki, K., Suzuki, K., and Yamamoto, K., 2004, Applications of T-lymphoma labeled with fluorescent quantum dots to cell tracing markers in mouse body, *Biochem. Biophys. Res. Commun*. 314:46–53.

Jaiswal, J.K., Mattoussi, H., Mauro, J.M., and Simon, S.M., 2003, Long-term multiple color imaging of live cells using quantum dot bioconjugates, *Nat. Biotechnol*. 21:47–51.

Jericevic, Z., Wiese, B., Bryan, J., and Smith, L.C., 1989, Validation of an imaging system: Steps to evaluate and validate a microscope imaging system for quantitative studies, *Methods Cell Biol*. 30:47–83.

Ji, J., Rosenzweig, N., Jones, I., and Rosenzweig, Z., 2002, Novel fluorescent oxygen indicator for intracellular oxygen measurements, *J. Biomed. Opt.* 7:404–409.

Kahana, J., and Silver, P., 1996, Use of the A. victoria green fluorescent protein to study protein dynamics in vivo, In: *Current Protocols in Molecular Biology* (F.M. Ausabel, R. Brent, R.E. Kingston, D.D. Moore, J.G. Seidman, J.A. Smith, K. Struhl, eds.), John Wiley and Sons, New York, pp. 9.7.22–9.7.28.

Kang, H.C., Fisher, P.J., Prendergast, F.G., and Haugland, R.P., 1988, Bodipy: A novel fluorescein and NBD substitute, *J. Cell Biol.* 107:34a.

Kao, J.P.Y., Harootunian, A.T., and Tsien, R.Y., 1989, Photochemically generated cytosolic calcium pulses and their detection by fluo-3. *J. Biol. Chem*. 264:8179–8184.

Kaplan, N.O., 1960, The pyridine coenzymes, In: *The Enzymes*, 2nd ed. (P.D. Boyer, H. Lardy, K. Myrbäck, eds.), Academic Press, New York, pp. 105–169.

Kneen, M., Farinas, J., Li, Y., and Verkman, A.S., 1998, Green fluorescent protein as a noninvasive intracellular pH indicator, *Biophys. J*. 74:1591–1599.

Koziol, J., 1971, Fluorometric analyses of riboflavin and its coenzymes, *Methods Enzymol*. 18B:253–285.

Kurtz, I., and Balaban, R.S., 1985, Fluorescence emission spectroscopy of 1,4-dihydroxyphthalonitrile: A method for determining intracellular pH in cultured cells, *Biophys. J*. 48:499–508.

Kurtz, I., and Emmons, C., 1993, Measurement of intracellular pH with a laser scanning confocal microscope, In: *Methods in Cell Biology 38: Cell Biological Applications of Confocal Microscopy* (B. Matsumoto, ed.), Academic Press, San Diego, California.

Kuwahara, M., and Verkman, A.S., 1988, Direct fluorescence measurement of diffusional water permeability in the vasopressin-sensitive kidney collecting tubule, *Biophys. J.* 54:587–593.

Kuwahara, M., Berry, C.A., and Verkman, A.S., 1988, Rapid development of vasopressin-induced hydroosmosis in kidney collecting tubules measured by a new fluorescence technique, *Biophys. J.* 54:595–602.

Labas, Y.A., Gurskaya, N.G., Yanushevich, Y.G., Fradkov, A.F., Lukyanov, K.A., Lukyanov, S.A., and Matz, M.V., 2002, Diversity and evolution of the green fluorescent protein family, *Proc. Natl. Acad. Sci. USA* 99:4256–4261.

Lakowicz, J.R., 1983, Fluorescence lifetime imaging, *Anal. Biochem*. 202:316–330.

Lakowicz, J.R., 1989, *Principles of Fluorescence Spectroscopy*, 2nd ed., Kluwer Academic, Plenum Press, New York.

Lewis, G.N., Lipkin, D., and Magel, T.T., 1941, Reversible photochemical processes in rigid media. A study of the phosphorescent state, *J. Am. Chem. Soc*. 63:3005–3018.

Li, L., Szmacinski, H., and Lakowicz, J.R., 1997, Synthesis and luminescence spectral characterization of long-lifetime lipid metal-ligand probes, *Anal. Biochem*. 244:80–85.

Lindqvist, L., 1960, A flash photolysis study of fluorescein, *Arkiv. Kemi.* 16:79–138.

Liphardt, B., Liphardt, B., and Lüttke, W., 1982, Laserfarbstoffe mit intramolekularer Triplettlöschung, *Chemische Berichte* 115:2997–3010.

Liphardt, B., Liphardt, B., and Lüttke, W., 1983, Laser dyes III: Concepts to increase the photostability of laser dyes, *Opt. Commun*. 48:129–133.

Lippincott-Schwartz, J., and Patterson, G.H., 2003, Development and use of fluorescent protein markers in living cells, *Science* 300:87–91.

Lippincott-Schwartz, J., Altan-Bonnet, N., and Patterson, G.H., 2003, Photobleaching and photoactivation: following protein dynamics in living cells, *Nat. Cell Biol. Suppl*. S7–S14.

Lippincott-Schwartz, J., Presley, J.F., Zaal, K.J., Hirschberg, K., Miller, C.D., and Ellenberg, J., 1999, Monitoring the dynamics and mobility of membrane proteins tagged with green fluorescent protein, *Methods Cell Biol*. 58:261–281.

Lippincott-Schwartz, J., Snapp, E., and Kenworthy, A., 2001, Studying protein dynamics in living cells, *Nat. Rev. Mol. Cell Biol.* 2:444–456.

Llopis, J., McCaffery, J.M., Miyawaki, A., Farquhar, M.G., and Tsien, R.Y., 1998, Measurement of cytosolic, mitochondrial, and Golgi pH in single living cells with green fluorescent proteins, *Proc. Natl. Acad. Sci. USA* 95:6803–6808.

Loew, L.M., 1993, Confocal microscopy of potentiometric fluorescent dyes, In: *Methods in Cell Biology 38:Cell Biological Applications* (B. Matsumoto, ed.), Academic Press, San Diego, California, pp. 195–209.

Manitto, P., Speranza, G., Monti, D., and Gramatica, P., 1987, Singlet oxygen reactions in aqueous solution. Physical and chemical quenching rate constants of crocin and related carotenoids, *Tetrahedron Lett.* 28: 4221–4224.

March, J.C., Rao, G., and Bentley, W.E., 2003, Biotechnological applications of green fluorescent protein, *Appl. Microbiol. Biotechnol*. 62:303–315.

Marriott, G., Clegg, R.M., Arndt-Jovin, D.J., and Jovin, T.M., 1991, Time-resolved imaging studies. Phosphorescence and delayed fluorescence imaging, *Biophys. J.* 60:1374–1387.

Matheson, I.B.C., and Rodgers, M.A.J., 1982, Crocetin, a water soluble carotenoid monitor for singlet molecular oxygen, *Photochem. Photobiol*. 36:1–4.

Mathies, R.A., and Stryer, L., 1986, Single-molecule fluorescence detection: A feasibility study using phycoerythrin, In: *Applications of Fluorescence in the Biomedical Sciences* (D.L. Taylor, A.S. Waggoner, R.F. Murphy, F. Lanni, R.R. Birge, eds.), Alan R. Liss, New York, pp. 129–140.

Matthews, M.M., and Sistrom, W.R., 1959, Function of carotenoid pigments in nonphotosynthetic bacteria, *Nature (Lond.)* 184:1892–1893.

Matz, M.V., Lukyanov, K.A., and Lukyanov, S.A., 2002, Family of the green fluorescent protein: Journey to the end of the rainbow, *BioEssays* 24:953–959.

Meyer, T., and Teruel, M.N., 2003, Fluorescence imaging of signaling networks, *Trends Cell Biol.* 13:101–106.

Minta, A., Kao, J.P.Y., and Tsien, R.Y., 1989, Fluorescent indicators for cytosolic calcium based on rhodamine and fluorescein chromophores, *J. Biol. Chem*. 264:8171–8178.

Misteli, T., and Spector, D.L., 1997, Applications of the green fluorescent protein in cell biology and biotechnology, *Nat. Biotechnol*. 15:961–964.

Miyawaki, A., 2002, Green fluorescent protein-like proteins in reef Anthozoa animals, *Cell Struct. Funct.* 27:343–347.

Miyawaki, A., 2003, Fluorescence imaging of physiological activity in complex systems using GFP-based probes, *Curr. Opin. Neurobiol*. 13:591–596.

Miyawaki, A., and Tsien, R.Y., 2000, Monitoring protein conformations and interactions by fluorescence resonance energy transfer between mutants of green fluorescent protein, *Methods Enzymol*. 327:472–500.

Miyawaki, A., Griesbeck, O., Heim, R., and Tsien, R.Y., 1999, Dynamic and quantitative Ca2+ measurements using improved chameleons, *Proc. Natl. Acad. Sci. USA* 96:2135–2140.

Miyawaki, A., Llopis, J., Heim, R., *et al.*, 1997, Fluorescent indicators for Ca^{2+} based on green fluorescent proteins and calmodulin, *Nature* 388:882–887.

Miyawaki, A., Sawano, A., and Kogure, T., 2003, Lighting up cells: Labelling proteins with fluorophores. *Nat. Cell Biol.* 5(Suppl):S1–S7.

Mujumdar, R.B., Ernst, L.A., Mujumdar, S.R., Lewis, C.J., and Waggoner, A.S., 1993, Cyanine dye labeling reagents: Sulfoindocyanine succinimidyl esters, *Bioconjug. Chem.* 4:105–111.

Mukkala, V.M., 1993, Development of stable, photoluminescent Europium (III) and Terbium (III) chelates suitable as markers in bioaffinity assays: Their synthesis and luminescence properties, PhD thesis, University of Turku, Turku, Finland.

Nagai, T., Sawano, A., Park, E.S., and Miyawaki, A., 2001, Circularly permuted green fluorescent proteins engineered to sense Ca^{2+}, *Proc. Natl. Acad. Sci. USA* 98:3197–3202.

Nagai, T., Yamada, S., Tominaga, T., Ichikawa, M., and Miyawaki, A., 2004, Expanded dynamic range of fluorescent indicators for Ca(2+) by circularly permuted yellow fluorescent proteins, *Proc. Natl. Acad. Sci. USA* 101:10554–10559.

Nakanishi, J., Maeda, M., and Umezawa, Y., 2004, A new protein conformation indicator based on biarsenical fluorescein with an extended benzoic acid moiety, *Anal. Sci*. 20:273–278.

Nguyen, D.C., Keller, R.A., Jett, J.H., and Martin, J.C., 1987, Detection of single molecules of phycoerythrin in hydrodynamically focused flows by laser-induced fluorescence, *Anal. Chem*. 59:2158–2161.

Niswender, K.D., Blackman, S.M., Rohde, L., Magnuson, M.A., and Piston, D.W., 1995, Quantitative imaging of green fluorescent protein in cultured cells: Comparison of microscopic techniques, use in fusion proteins and detection limits, *J. Microsc*. 180:109–116.

Oi, V., Glazer, A.N., and Stryer, L., 1982, Fluorescent phycobiliprotein conjugates for analyses of cells and molecules, *J. Cell Biol*. 93:981–986.

Oswald, B., Duschl, J., Patsenker, L., Wolfbeis, O.S., and Terpetschnig, E., 1999, Synthesis, spectral properties, and detection limits of reactive squaraine dyes, a new class of diode laser compatible fluorescent protein labels, *Bioconjug. Chem.* 10:925–931.

Panchuk-Voloshina, N., Haugland, R.P., Bishop-Stewart, J., Bhalgat, M.K., Millard, P.J., Mao, F., Leung, W.-Y., and Haugland, R.P., 1999, Alexa dyes, a series of new fluorescent dyes that yield exceptionally bright, photostable conjugates, *J. Histochem. Cytochem*. 47:1179–1188.

Patterson, G., Day, R.N., and Piston, D., 2001, Fluorescent protein spectra, *J. Cell Sci*. 114:837–838.

Patterson, G.H., Knobel, S.M., Sharif, W.D., Kain, S.R., and Piston, D.W., 1997, Use of the green-fluorescent protein (GFP) and its mutants in quantitative fluorescence microscopy, *Biophys. J.* 73:2782–2790.

Peck, K., Stryer, L., Glazer, A.N., and Mathies, R.A., 1989, Single molecule fluorescence detection: Autocorrelation criterion and experimental realization with phycoerythrin, *Proc. Natl. Acad. Sci. USA*, 86:4087–4091.

Phillips, G.N., 1999, Structure and dynamics of green fluorescent protein, *Curr. Opin. Struc. Biol*. 7:821–827.

Piston, D.W., Patterson, G.H., and Knobel, S.M., 1999, Quantitative imaging of the green fluorescent protein (GFP), *Methods Cell Biol*. 58:31–47.

Prasher, D.C., Eckenrode, V.K., Ward, W.W., Prendergast, F.G., and Cormier, M.J., 1992, Primary structure of the Aequorea victoria green-fluorescent protein, *Gene* 111:229–233.

Rechtenwald, D.J., 1989, US Patent 4,876,190.

Reits, E.A., and Neefjes, J.J., 2001, From fixed to FRAP: Measuring protein mobility and activity in living cells, *Nat. Cell Biol.* 3:E145–E147.

Reyftmann, J.P., Kohen, E., Morliere, P., Santus, R., Kohen, C., Mangel, W.F., Dubertret, L., and Hirschberg, J.G., 1986, A microspectrofluorometric study of porphyrin-photosensitized single living cells — I. Membrane alterations, *Photochem. Photobiol*. 44:461–469.

Richieri, G.V., Ogata, R.T., and Kleinfeld, A.M., 1992, A fluorescently labeled intestinal fatty acid binding protein, *J. Biol. Chem*. 267:23495–23501.

Richieri, G.V., Anel, A., and Kleinfeld, A.M., 1993, Interactions of long-chain fatty acids and albumin: Determination of free fatty acid levels using the fluorescent probe ADIFAB, *Biochemistry* 32:7574–7580.

Rizzuto, R., Brini, M., Pizzo, P., Murgia, M., and Pozzan, T., 1995, Chimeric green fluorescent protein (GFP): A new tool for visualizing subcellular organelles in living cells, *Curr. Biol.* 5:635–642.

Roederer, M., Kantor, A.B., Parks, D.R., and Herzenberg, L.A., 1996, Cy7PE and Cy7APC: Bright new probes for immunofluorescence, *Cytometry* 24:191–197.

Rye, H.S., Yue, S., Wemmer, D.E., Quesada, M.A., Haugland, R.P., Mathies, R.A., and Glazer, R.N., 1992, Stable fluorescent complexes of double-stranded DNAs with bis-intercalating asymmetrical cyanine dyes: Properties and applications, *Nucleic Acids Res*. 20:2803–2812.

Sacchetti, A., Ciccocioppo, R., and Alberti, S., 2000, The molecular determinants of the efficiency of green fluorescent protein mutants, *Histol. Histopathol*. 15:101–107.

Schäfer, F.P., 1983, New developments in laser dyes, *Laser Chem*. 3:265–278.

Schneider, M.B., and Webb, W.W., 1981, Measurement of submicron laser beam radii, *Appl. Opt*. 20:1382–1388.

Seveus, L., Vaisala, M., Hemmlia, I., Kojola, H., Roomans, G.M., and Soini, E., 1994, Use of fluorescent Europium chelates as labels in microscopy allows glutaraldehyde fixation and permanent mounting and leads to reduced autofluorescence and good long-term stability, *Microsc. Res. Techn*. 28:149–154.

Sheetz, M.P., and Koppel, D.E., 1979, Membrane damage caused by irradiation of fluorescent concanavalin A, *Proc. Natl. Acad. Sci. USA* 76:3314–3317.

Smith, S.J., and Augustine, G.J., 1988, Calcium ions, active zones and synaptic transmitter release, *Trends Neurosci*. 11:458–464.

Smith, P.J., Blunt, N., Wiltshire, M., Hoy, T., Teesdale-Spittle, P., Craven, M.R., Watson, J.V., Amos, W.B., Errington, R.J., and Patterson, L.H., 2000, Characteristics of a novel deep red/infrared fluorescent cell-permeant DNA probe, DRAQ5, in intact human cells analyzed by flow cytometry, confocal and multiphoton microscopy, *Cytometry* 40(4):280–291.

Snyder, D.S., Garon, C.F., 2003, Decreased uptake of bodipy-labelled compounds in the presence of the nuclear stain, DRAQ5, *J. Microsc.* 211(Pt 3):208–211.

Soini, E.J., Pelliniemi, L.J., Hemmila, I.A., Mukkala, V.-M., Kankare, J.J., and Froidman, K., 1988, Lanthanide chelates as new fluorochrome labels for cytometry, *J. Histochem. Cytochem*. 36:1449–1451.

Southwick, P.L., Ernst, L.A., Tauriello, E.W., Parker, S.R., Mujumdar, R.B., Mujumdar, S.R., Clever, H.A., and Waggoner, A.S., 1990, Cyanine dye labeling reagents — Carboxymethylindocyanine succinimidyl esters, *Cytometry* 11:418–430.

Stearns, T., 1995, Green fluorescent protein — The green revolution, *Curr. Biol*. 5:262–264.

Strickler, S.J., and Berg, R.A., 1962, Relationship between absorption intensity and fluorescence lifetime of molecules, *J. Chem. Phys*. 37:814–822.

Sullivan, K.F., and Kay, S.A., 1999, *Green Fluorescent Proteins*, Academic Press, San Diego, California.

Sun, C., Yang, J., Li, L., Wu, X., Liu, Y., and Liu, S., 2004, Advances in the study of luminescence probes for proteins, *J. Chromat. B: Anal. Technol. Biomed. Life Sci*. 803:173–190.

Sun, L., Wang, S., Chen, L., and Gong, X., 2003, Promising fluorescent probes from phycobiliproteins, *IEEE J Select. Topics Quant. Electron*. 9:177–188.

Tinoco, I., Mickols, W., Maestre, M.F., and Bustamante, C., 1987, Absorption, scattering, and imaging of biomolecular structures with polarized light, *Annu. Rev. Biophys. Biophys. Chem*. 16:319–349.

Trask, B.J., 1991, DNA sequence localization in metaphase and interphase cells by fluorescence in situ hybridization, *Methods Cell Biol*. 35:1–35.

Tsien, R.Y., 1988, Fluorescence measurement and photochemical manipulation of cytosolic free calcium, *Trends Neurosci*. 11:419–424.

Tsien, R.Y., 1989a, Fluorescent probes of cell signaling, *Annu. Rev. Neurosci*. 12:227–253.

Tsien, R.Y., 1989b, Fluorescent indicators of ion concentrations, *Methods Cell Biol*. 30:127–156.

Tsien, R.Y., 1998, The green fluorescent protein, *Annu. Rev. Biochem*. 67:509–544.

Tsien, R.Y., 2003, Imagining imaging's future, *Nat. Rev. Mol. Cell Biol*. 4(Suppl):SS16–SS21.

Tsien, R.Y., and Miyawaki, A., 1998, Seeing the machinery of live cells, *Science* 280:1954–1955.

Tsien, R.Y., and Poenie, M., 1986, Fluorescence ratio imaging: A new window into intracellular ionic signaling, *Trends Biochem. Sci*. 11:450–455.

Uster, P.S., and Pagano, R.E., 1986, Resonance energy transfer microscopy: Observations of membrane-bound fluorescent probes in model membranes and in living cells, *J. Cell Biol*. 103:122–124.

van Roessel, P., and Brand, A.H., 2002, Imaging into the future: visualizing gene expression and protein interactions with fluorescent proteins, *Nat. Cell Biol*. 4:E15–E20.

Vereb, G., Jares-Erijman, E., Selvin, P.R., and Jovin, T.M., 1998, Temporally and spectrally resolved imaging microscopy of lanthanide chelates, *Biophys. J*. 74:2210–2222.

Verkhusha, V.V., and Lukyanov, K.A., 2004, The molecular properties and applications of Anthozoa fluorescent proteins and chromoproteins, *Nat. Biotechnol*. 22:289–296.

Viallet, P.M., and Vo-Dinh, T., 2003, Monitoring intracellular proteins using fluorescence techniques: From protein synthesis and localization to activity, *Curr. Protein Peptide Sci*. 4:375–388.

Vigers, G.P.A., Coue, M., and McIntosh, J.R., 1988, Fluorescent microtubules break up under illumination, *J. Cell Biol*. 107:1011–1024.

Voura, E.B., Jaiswal, J.K., Mattoussi, H., and Simon, S.M., 2004, Tracking metastatic tumor cell extravasation with quantum dot nanocrystals and fluorescence emission-scanning microscopy, *Nat. Med*. 10:993–998.

Wages, J., Packard, B., Edidin, M., and Brand, L., 1987, Time-resolved fluorescence of intracellular quin-2, *Biophys. J*. 51:284a.

Waggoner, A., DeBiasio, R., Conrad, P., Bright, G.R., Ernst, L., Ryan, K., Nederlof, M., and Taylor, D., 1989, Multiple spectral parameter imaging, *Methods Cell Biol*. 30:449–478.

Waggoner, A.S., Ernst, L.A., Chen, C.-H., and Rechtenwald, D.J., 1993, A new fluorescent antibody label for three-color flow cytometry with a single laser, *Ann. N.Y. Acad. Sci*. 677:185–193.

Wahlfors, J., Loimas, S., Pasanen, T., and Hakkarainen, T., 2001, Green fluorescent protein (GFP) fusion constructs in gene therapy research, *Histochem. Cell Biol*. 115:59–65.

Ward, W.W., Cody, C.W., and Hart, R.C., 1980, Spectrophotometric identity of the energy transfer chromophores in Renilla and Aequorea green-fluorescent proteins, *Photochem. Photobiol*. 31:611–615.

Watt, R.M., and Voss, E.W. Jr., 1977, Mechanism of quenching of fluorescein by anti-fluorescein IgG antibodies, *Immunochemistry* 14:533–541.

Weijer, C.J., 2003, Visualizing signals moving in cells, *Science 300*:96–100.

Wessendorf, M.W., and Brelje, T.C., 1992, Which fluorophore is brightest? A comparison of the staining obtained using fluorescein, tetramethylrhodamine, lissamine rhodamine, Texas Red, and cyanine 3.18, *Histochemistry* 98:81–85.

White, J.C., and Stryer, L., 1987, Photostability studies of phycobiliprotein fluorescent labels, *Anal. Biochem*. 161:442–452.

White, J.G., Amos, W.B., and Fordham, M., 1987, An evaluation of confocal versus conventional imaging of biological structures by fluorescence light microscopy, *J. Cell Biol*. 105:41–48.

Wilson, E.O., 1975, *Sociobiology*, Harvard University Press, Cambridge, Massachusetts, pp. 38–43.

Wories, H.J., Koek, J.H., Lodder, G., Lugtenburg, J., Fokkens, R., Driessen, O., and Mohn, G.R., 1985, A novel water-soluble fluorescent probe: synthesis, luminescence and biological properties of the sodium salt of the 4-sulfonato-3,3′,5,5′-tetramethyl-2,2′-pyrromethen-1,1′-BF_2 complex, *Recl. Trav. Chim. Pays-Bas* 104:288–291.

Yip, K.-P., and Kurtz, I., 2002, Confocal fluorescence microscopy measurements of pH and calcium in living cells, *Methods Cell Biol*. 70:417–427.

Yu, H., Ernst, L.A., Wagner, M., and Waggoner, A.S., 1992, Sensitive detection of RNAs in single cells by flow cytometry, *Nucleic Acids Res*. 20:83–88.

Zaccolo, M., and Pozzan, T., 2000, Imaging signal transduction in living cells with GFP-based probes. IUBMB, *Life* 49:375–379.

Zacharias, D.A., 2002, Sticky caveats in an otherwise glowing report: Oligomerizing fluorescent proteins and their use in cell biology, *Sci. STKE* 2002:E23.

Zacharias, D.A., Baird, G.S., and Tsien, R.Y., 2000, Recent advances in technology for measuring and manipulating cell signals, *Curr. Opin. Neurobiol*. 10:416–421.

Zhang, J., Campbell, R.E., Ting, A.Y., and Tsien, R.Y., 2002, Creating new fluorescent probes for cell biology, *Nat. Rev. Mol. Cell Biol*. 3:906–918.

Zimmer, M., 2002, Green fluorescent protein (GFP): Applications, structure, and related photophysical behavior, *Chem. Rev*. 102:759–781.